

Study of Mechanical Properties and Applications of Aluminium Based Composites Manufactured Using Laser Based Additive Techniques



Sumit Choudhary  and Vidit Gaur 

Abstract Today, Laser-based additive manufacturing is the most adaptable and promising technology for the fabrication of complex design light weight composite components. This chapter explores the laser-based additive techniques and the factors that make them superior compared to conventional techniques. Both the in-situ and ex-situ reinforced metal matrix composites can be manufactured using additive manufacturing efficiently and can achieve higher mechanical properties compared to conventionally manufacture. Some reinforcing materials such as ZBr_2 , AlN, SiC, Al_2O_3 , HEAs, and CNTs may help to make the aluminium based light weight composites a promising candidate for almost all the industrial engineering sectors. In the future, additive manufacturing may be used to fabricate new Aluminium alloys series (2XXX, 5XXX, 6XXX and 7XXX) for manufacturing new composites by reinforcing nanomaterials and controlling the process parameters.

Keywords Laser-based additive manufacturing · Composites · Mechanical properties

1 Introduction

Over the last few decades, the demands of modern industries increase rapidly for lightweight, high-performance materials having magnificent mechanical properties. In aerospace and automotive engineering, lightweight metallic materials (Aluminium and titanium) are a major concern, but advanced development is required because of poor strength and low hardness [1]. Nevertheless, these materials can become a promising candidate for industrial applications by reinforcing them through ceramic particles, Carbon Nano Tubes (CNTs), High entropy alloys particles, and Graphene Nanoplatelets (GNPs), etc. These reinforcing materials have remarkably

S. Choudhary · V. Gaur (✉)

Department of Mechanical and Industrial Engineering, Indian Institute of Technology Roorkee, Roorkee 247667, India

e-mail: vidit.gaur@me.iitr.ac.in

© The Author(s), under exclusive license to Springer Nature Singapore Pte Ltd. 2022

261

A. Praveen Kumar et al. (eds.), *High-Performance Composite Structures*,

Composites Science and Technology,

https://doi.org/10.1007/978-981-16-7377-1_12

high mechanical properties, superior thermal properties, and extraordinary electrical properties along with some other exceptional properties like relatively low density, superior hardness, and a very low coefficient of thermal expansion [1, 2]. For a long time, a wide class of conventional manufacturing methods are used for fabricating lightweight metal matrix composites based on their processing temperatures like squeeze casting, stir casting, melt infiltration, reaction infiltration for liquid phase processing. For solid-phase processing, some conventional methods such as pressing and sintering, diffusion bonding, friction stir welding, forging, and extrusion [3]. Sometimes, in-situ reinforcement was also performed using different casting processes to fabricate lightweight composites [4]. However, the conventional methods have some limitations, such as the constraint on complex geometry and the agglomeration of reinforcing materials, which may cause non-uniformity in the microstructure of the grains [5].

Moreover, some materials are stable in the liquid phase. But during solidification, they became unstable and formed some undesired phases like intermetallic and laves within the composite matrix, which completely deteriorates the mechanical properties of the composite [6]. Therefore, Additive manufacturing was developed and has proven design freedom with time, making it an excellent material processing technique having the capabilities to fabricate any design geometry that humans can think of [7]. Additive manufacturing also suppressed the agglomeration problem with the help of manipulating the process parameters and adding reinforced materials [8]. The reinforced materials are incorporated in the matrix either ex-situ or in-situ. When these reinforced particles interact with the matrix material during the melting and solidification, they get very short period, due to which they do not segregate or agglomerate [9].

Recently, in the COVID-19 pandemic, additively manufactured products are currently being used by patients and front-line workers in hospitals, such as face shields, face masks, nebulizers. These products are diversely designed due to emergencies [10]. However, some medical devices like the charlotte valve, venture valve, snorkeling mask, nasopharyngeal swab, portable oxygen cylinder kit, and oxygen concentrator components require strict design standards. Therefore, some insights into additive manufacturing based on material and processing parameters are still needed to mitigate the future requirements [11]. This technology even opens new doors in the field of space technology, giants like SpaceX, GE, NASA, ISRO, and Skyroot Aerospace (100% 3D printed Dhawan-1 rocket engine [12]) industries continuously promote and develop additively manufactured small and medium-size components like fuel injectors, nozzles, diffusers guiding vanes and some other hot-section components in the spacecraft, and also testing entirely 3D printed cryogenic engines for future applications [13, 14]. The automobile industries are continuously testing and developing additively manufactured components such as turbochargers, alloy wheels, brake line holders, hose holders, and chassis components for racing cars and regular vehicles to improve the overall efficiency by weight reduction without compromising the strength [15, 16]. Additive manufacturing also helps in reducing the inventory of spare parts in the automobile industry [17].

Moreover, AM is tremendously used in bio-implants applications to fabricate the light composites of titanium and biodegradable magnesium alloys [18, 19]. AM is very popular for bio-implants because of its potential to create complex geometries and tailor the implant's mechanical properties [20]. Recently, 3D Systems has been launched the latest hybrid maxillofacial surgical guide to its Computer-generated Surgical Planning service in that they train dentists about 3D printed dental implants [21].

Additive manufacturing techniques like Selective Laser Melting (SLM), Selective Laser Sintering (SLS), and Electron beam Melting (EBM) are some of today's most exploited techniques. The industries are also incorporate these techniques because of design freedom, time-saving, and cost-effectiveness. In addition to that, they have the capabilities to use any material for fabrication, which either be a ceramic, metal, polymer, and can be in any phase either in solid, liquid, or powder form [22]. Moreover, AM can easily tailor the component's properties and can be easily controlled by varying the process parameters, matrix material, and reinforcement materials. The combination of these three primary things can be used to tailor the microstructure of grains that finally provide the tailored properties [23]. In most of the aluminium based composites fabricated by the AM, mechanical properties, wear resistance, and corrosion resistance are improved after the reinforcement [24–26]. So far, only conventional techniques are used for the manufacturing of lightweight composites. However, in this chapter, the novelty found in different studies of additively manufactured lightweight composites are tried to present collectively to design a better plan for future development in the same field.

Furthermore, some aluminium alloys and their composites which come under the category of high strength alloys, strain hardened such as 2000, 5000, 6000, and 7000 series, are still far away from the reach of laser-based additive manufacturing. Because these alloys having a problem of cracking during solidification (or hot tearing) and also contains some alloying elements which are volatile at processing temperature [27, 28]. However, this problem can be reduced in future research by reinforcing some suitable materials, optimizing the process parameters, or developing some more new techniques. By combining all the capabilities and future aspects of laser-based additive manufacturing, the lightweight MMCs components can become the most promising candidates to encounter the challenges of the industries such as healthcare (bio-implants and other equipment), automotive, and aerospace, etc. So, in the next heading discussion about the origin of additive manufacturing and how it works is elaborated.

2 Additive Manufacturing Processes

In 1984 UVP, Inc. granted a patent US45755330, which is later allotted to the Chuck Hull (3D Systems Corporation) for the stereolithography fabrication system, which shows the capabilities of adding a layer by layer way to fabricate the components [29]. The hull's contributed the STL (Stereolithography) file format, which is even today



Fig. 1 Simple flow chart of the complete additive manufacturing process

used to slice the digital (CAD) drawing for additive manufacturing (AM) machine. Later Hull's commercialize his first 3D printer (SLA-1) [30]. Many technologies are available in the market, which are used to fabricate the components additively, like rapid prototyping (RP), layered manufacturing (LM), additive manufacturing, 3-dimensional printing (3DP), and solid freeform fabrication (SFF), etc. In additive manufacturing, the material is added in a layer-by-layer manner in three-dimensions which finally create the same product as fed by the computer design, thus the process called additive manufacturing [31]. In simple words, additive manufacturing is just the reverse of subtractive manufacturing processes like shaping and milling. A simple flow chart of the complete process is schematically revealed in Fig. 1.

Additive manufacturing can be used to fabricate almost all categories of materials, whether metals, polymers, and ceramics, along with the combinations of them like metal matrix composites (MMCs), Polymer matrix composites (PMCs), and their functionally graded materials (FGMs). The reinforcing elements can also belong to any category of metals, ceramics, and polymers.

The freedom of design developed by the AM process even makes it more powerful to fabricate any complicated geometric design. This powerful feature makes it the need of future technology, and it's rapidly becoming mature day by day. Even in today's time, this technology is used in almost all areas. In contrast, conventional manufacturing techniques don't have freedom of design, and wastage is high, which means high cost. The broad comparison of different factors is discussed in the next section.

3 Additive Manufacturing Versus Conventional Manufacturing

AM has removed all the barriers from fabrication processes. Today Engineers can design and customize anything without worried about fabrication constraints. The mechanical properties can easily be tailored in a required orientation by controlling the process parameters and the raw material composition. While in conventional techniques, it is almost impossible to manipulate the required properties according to the design requirements. The AM nowadays is also used for repairing the purpose of failure components, as shown in Fig. 2b. The functionally graded Materials (FGMs) components are easy and cheap to fabricate using AM just by changing the feedstock mechanism. The porous material used for bio-implants, drug delivery, and tissue engineering can easily be manufactured by the AM, as shown in Fig. 2a. Moreover, AM

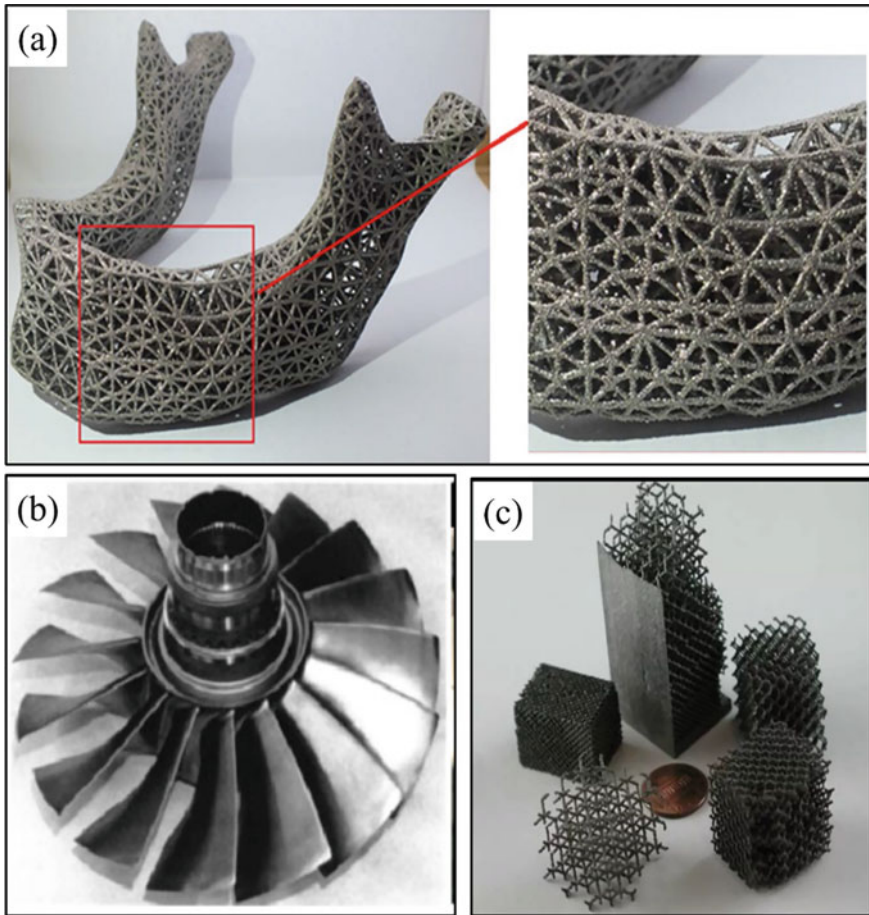


Fig. 2 a EBM technology used to fabricate a 3D mesh titanium mandibular prosthesis scaffold. b Directed energy deposition process used to repair damaged blisk c using EBM Lattice-structured Ti6Al4V foams was built. Adapted from Liu [32]

gives a new opportunity to fabricate lightweight composite materials for structures with complex geometries, see Fig. 2c.

The fabrication of structure of multi-directional composites are now become very easy because of optimization of design parameters and to manufacture prototype by iteration of process parameters. The summary of the comparisons between AM and conventional techniques is shown in Table 1.

Before discussing the classification of additive manufacturing, let's discuss some of its important parameters that affect the final product's properties.

Table 1 The collection of comparison factors between AM and traditional techniques

Factor	Additive manufacturing	Conventional manufacturing
Product complexity	Developed to fabricate any imagined geometric complex product	Challenging to fabricate complex geometries. The complex parts are manufactured separately and assemble
Post Processing	Post-processing depends upon the material and process used for fabrication. Polymer-based fabrication mostly doesn't require any post-processing However the metal and ceramic-based composites require very little post-processing	Almost all the fabricated products require some kind of post-processing
Resource utilization	The optimized quantity of resources is consumed because the final product is fabricated directly from the CAD design	Consumption is very high because at each stage, from design to final product, the resources are consumed in much higher amount
Material consumption	Almost no wastage of raw material because of optimization of design and fabrication process. The unprocessed material can easily be reused	Material wastage is very high due to the requirement of post-processing and the complex geometries manufactured separately
Prototyping	Highly recommended for fabrication of the prototype. To quickly evaluate and perform iterations of design parameters	Not suggested for fabrication of prototype because of time-consuming and high expenditure
Cost	Most of the cost is utilized in optimizing the fabrication parameter for a material; once the parameters are optimized, the cost is less for small and medium batches production	These techniques are expansive for medium and small production batches because of the high consumption of resources, time, and post-processing
Time	It can fabricate the product in few minutes because it directly takes from the CAD model. These techniques also help in reducing inventory, controlling the supply chain, etc.	Time-taking techniques require the dyes, moulds, molten raw material, post-processing, and proper steps to fabricate the end products
Applications	Complex geometry components like Carburettors in Automobiles, Turbine blades, Bio implants, hot section components, etc.	Simple geometry components like casted engine blocks, casings, extruded parts, rods, I- sections, etc.

Adapted and modified from Fereiduni [1]

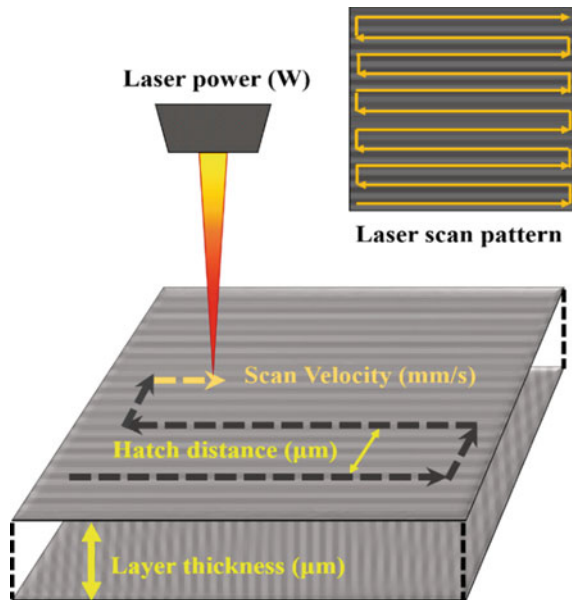
4 Some Important Parameters of Laser-Based Additive Manufacturing

In advanced laser-based additive manufacturing machines, hundreds of parameters are available such as laser selection, operational mode, laser energy density, vector length, beam spot size, scan angle, ratio of length to width, beam spatial distribution, point overlapping, laser wavelength, and pulsed or continuous operation [33]. However, the parameters generally considered are laser power, scan velocity, hatch distance, laser scan pattern, and layer thickness [34], as shown in Fig. 3. These general parameters are the majorly regulating parameters and will be discussed.

4.1 Laser Power

The laser power should be adjusted along with the laser spot to provide sufficient heat to melt or sinter the powders. To process the materials having high melting temperature, the laser of high energy density is required, which can be achieved by reducing the spot size by keeping the laser power same. It is the main parameter of processing because it decides the interaction between material and laser. So, its magnitude depends upon the kind of material that is processing. For polymers, it could be around 3–5 W, for metals in the range of 100–250 W, and for ceramics, it may go up to 500 W [35].

Fig. 3 Processing parameters of laser-based additive manufacturing



Moreover, laser power also depends on the layer thickness; as the layer thickness increases, more laser power is required to melt the powder properly. The accuracy of the fabricated part controlled by the size of the laser spot (30–600 μm); the smaller the size higher will be the accuracy [36]. Generally, for very complex designs, a tiny spot size is required. The laser-based machines are generally equipped with either CO_2 ($\lambda \approx 10.6 \mu\text{m}$) laser or Nd: YAG, Yb: YAG or Nd: YVO₄ ($\lambda \approx 1.06 \mu\text{m}$) lasers. The CO_2 laser mostly preferred for the oxides ceramics and the YAG laser for the metals and carbides ceramics [37]. The YAG laser machines give more accuracy than CO_2 laser because of the smaller laser spot size [38].

4.2 Scan Velocity

The rate at which the laser beam scans a powder strip (line) on the powder bed is called scan velocity. The fabrication rate or welding rate directly depends upon the scan velocity, higher the scan velocity higher will be the fabrication rate. Moreover, laser energy density also depends upon the scan velocity; the higher the scan velocity lower will be the laser energy density. So if scan velocity is higher, the energy density may not be sufficient to melt or fuse the material powder particles properly. Therefore to optimize the scan velocity generally, laser power, laser spot size, and laser energy density are considered in the calculation as given by the relation (1) [39].

$$\text{Laser energy density} = \frac{\text{laser power}}{\text{laser spot size} \times \text{scan velocity}} \quad (1)$$

It also depends upon the material to be processed. Generally, the scan velocity used during the process lies in the range of 0.1–15 mm/s. The chance of balling effect (Spheroidal beads) is more at higher scan velocity, which is explained by the Rayleigh instability to reduce the balling effect; high laser power and low scan velocity are suggested [35, 38, 40, 41].

4.3 Hatch Distance

The distance between the two adjacent melting strips/vector is known as hatch distance [42]. It mostly lies in the range of 20–400 μm . Generally, the laser spot size kept greater than the hatch distance because it decides the percentage of overlapping [38]. The overlapping is required to reduce the porosity because, in Gaussian beams, the power is concentrated at the laser beam centre. At the boundary, the less laser energy density causing in melting only at the centre portion remaining portion either partially melt or heated [34]. The hatch distance is also kept smaller when complex geometry components are fabricating. The fabrication rate also depends on

the hatch distance; the higher the hatch distance, the faster the fabrication or scanning rate [35].

4.4 Laser Scan Pattern

The way to scan the powder on the powder bed is commonly known as the laser scan pattern. It may be parallel lines, anti-parallel lines, lines at any specific angle (30°, 45°, 60°), or zigzag pattern. Fill and contour are the two most common categories of scan pattern; fill referred to the scanning across all over areas, and contour referred to the scanning at boundaries. The mechanical property, surface roughness, and defects of the final product are majorly depends upon it [43, 44]. Therefore it should be select according to the requirement of the final product properties.

In most cases, to remove the anisotropy and defects from the products, the scan direction changed by 90° in every sequential layer [35]. Moreover, to reduce shrinkage stresses, the scanning pattern of small islands can also be employed, which reduces the problem of localized heat build-up from larger areas and reduces thermal stresses and thermal cracks. In addition, to reduce the balling effect repeating scan pattern is preferred [41].

4.5 Layer Thickness

Layer thickness is the thickness of the powder recoated every time, followed by the processing of successive layers. This operation is done by reducing the height of the powder bed/build platform [35]. The thickness of the slice was defined in the CAD model is exactly equal to the layer thickness, which is physically converted by the feeder/recoater unit. The broad range of layer thickness lies under 30–300 μm [38]. Layer thickness is another crucial parameter directly related to mechanical properties, surface roughness, and fabrication speed. For higher accuracy components, the smaller layer thickness is preferred, but that increases fabricate time which means higher cost of the components and for bigger layer thickness the higher laser energy density is required. Therefore optimization of layer thickness is required by considering the laser energy density. The laser energy density is calculated by the given relation (2) [45].

$$\text{Laser energy density} = \frac{\text{laser power}}{\text{hatch distance} \times \text{scan velocity} \times \text{layer thickness}} \quad (2)$$

The smaller layer thickness can achieve a smoother surface and dimensional accuracy because the shrinkage after melting and defects will reduce significantly. Hence, better mechanical properties can be achieved. But the smaller size powder is

highly suggested for the smaller layer thickness and higher dimensional accuracy, which also improves the flow ability of the powder during recoating [35].

After discussing all the important parameters and their fundamental relations, the detailed classification is deliberated in the next section, along with a supporting flow chart and the figures.

5 Classifications of Additive Manufacturing Process

To Understand the AM in a better way ASTM committee has divided the techniques into different classes based on the basic principle of working, feedstock, power input, and applications [46]. The majority of the process fall into one of two groups, viz; (i) based on raw material state, i.e., solid (bulk), liquid or powder, and (ii) source used for the fusion of material on the molecular level, i.e., laser, electron beam, UV-light or thermal [13]. The AM processes that are often encountered are exposed in Fig. 4.

LBAM is an advanced manufacturing system; metal parts, polymers, composites, and functionally graded components can fabricate easily. In LBAM, the laser is employed to deliver the thermal energy for completely or partially melting of the additive material, and in the case of polymers, additive manufacturing laser (specific wavelength) is used to begin the chemical reaction in vat polymerization [47]. For LBAM, the initial state of material can be solid (metals, plastic), liquid (resins), and powder (metals, ceramics, and polymers) form [48]. For solids and liquids as a

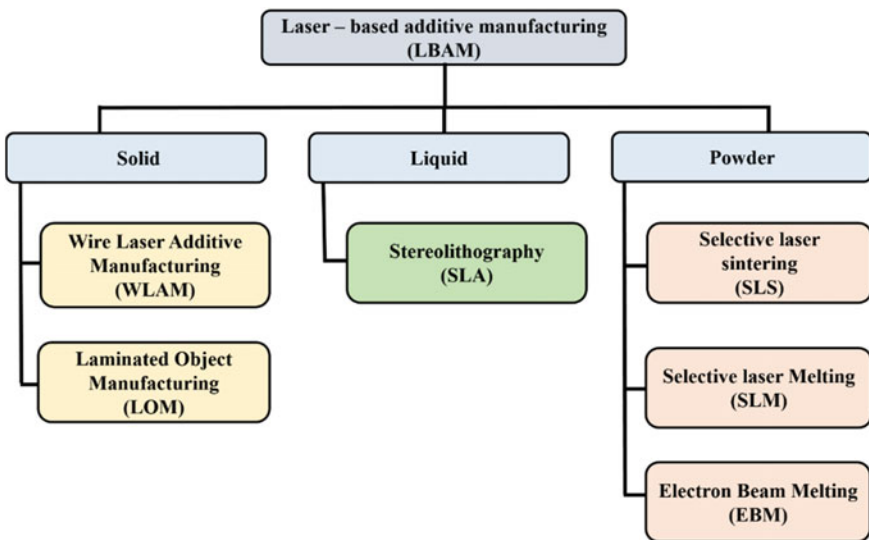


Fig. 4 Broader classifications of laser-based additive manufacturing

starting material, the AM processes commonly used are Wire Laser Additive Manufacturing (WLAM), Laminated Object Manufacturing (LOM) and, stereolithography (SLA), respectively [49]. Selective Laser Sintering (SLS), Selective Laser Melting (SLM), Electron Beam Melting (EBM) are the AM techniques considered to be best for Powder as an initial material [50]. Complete melting, limited melting (Solid-state sintering), liquid phase sintering, and chemically made binding are the molecular level fusion mechanisms of powder processes through LBAM. The overview of all the above listed LBAM is discussed in the following segment.

5.1 Wire Laser Additive Manufacturing (WLAM)

In WLAM, the melt pool on substrate material is generated by the high-intensity laser source, and the metal wire is fed as an additive material. The melted fed wire is bound to the substrate through metallurgical bonding. By the motion of laser gun head and wire feeder, i.e., welding tool unit, relative to the substrate, bead formation occurs during solidification, as shown in Fig. 5a. Generally, the robotic arm is used for WLAM, which provides the 6-axis relative motion between the substrate and welding tool, and this 6-axis relative motion help in fabricating the complex components accurately. Figure 5a also shows the bead formation along with real process images [51]. Before deposition, the process parameters are needed to be select and tune the equipment accordingly. Some important process parameters are the power of the laser (Voltage and current input), wire feed stock rate, and traverse speed of the welding tool. These parameters control the input of energy, rate of deposition, and beads cross-sectional profile (width and height) [52]. Moreover, wire diameter, wire/substrate angle, wire tip position with respect to the melt pool, and feeding direction are additional parameters needed to be carefully tuned to get stable deposition on a substrate. The volume of wire fed into the melt pool with respect to traversing speed and the laser power can be employed to determine the height of the bead [53, 54].

Figure 5b demonstrates that the deposition of specimen wall is smooth with minor irregularity; hence the chance of post-processing machining is lower. Figure 5c shows the geometric and metallurgy features of the wall cross-section. Regular shape geometry of the order of tens of mm scale is present [55].

5.2 Laminated Object Manufacturing (LOM)

In this technique, the paper and adhesive are used to fabricate the 3D object by consecutive layers of one side adhesive applied paper sheets. The geometry is achieved by cutting of laser, as shown in Fig. 6a, b. The rollers supply the building material, and other heated moving rollers are used to promote pressure and strengthen the interlayer bonding of adhesion applied paper sheets. The final part has properties similar to that

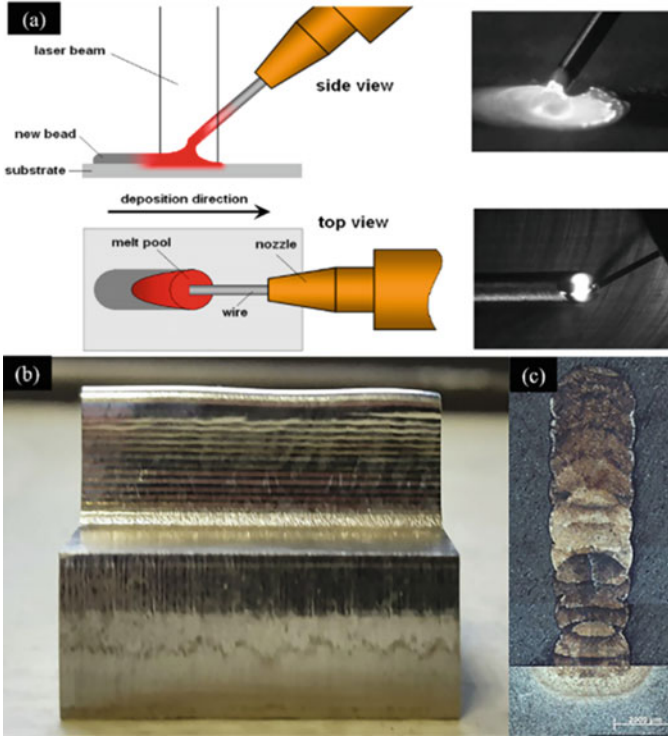


Fig. 5 a Left: Sketch of interaction between laser-wire, the relative motion of the fabrication tool and the substrate causes the molten metal to solidify into a bead. Right: view (top and side) of real process images adapted from Heralic [51]. b A demonstration wall after fabrication, and c cross-section image [55]

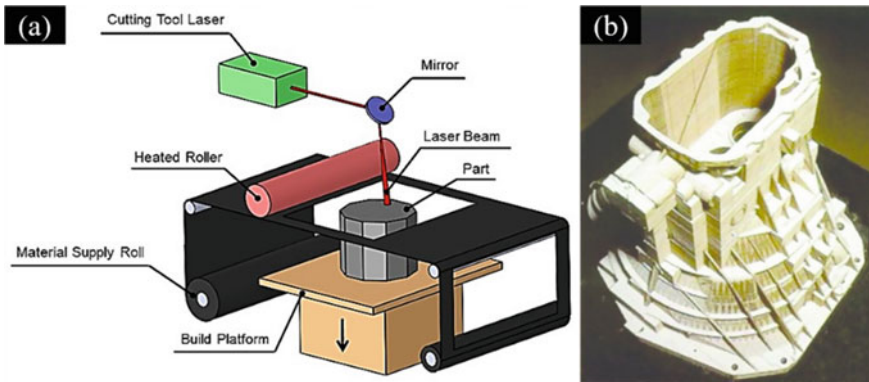


Fig. 6 a Schematic of Laminated Object Manufacturing setup adapted from Razavykia [58] b Sample of a model fabricated by LOM systems [59]

of wood, and the dimensional accuracy of 0.1 mm can be achieved [56]. LOM can also fabricate Polymer-based composites; in that case, the fiber reinforcement infiltrates the thermoplastic or thermoset polymer matrix through the melting and fusion, which finally imparts them interlayer bonding [57]. Ultrasonic Additive Manufacturing (UAM) is a category of LOM which combines both additive manufacturing and subtractive CNC milling operation to achieve the geometry of metallic components. The ultrasonic vibrations achieve solid-state atomic bonding by progressive downward force and motion with shallow heating. The CNC milling process is used to remove excess material [58].

LOM technique has some advantages like very economical and risk-free materials (paper, plastics.). The concept of process is simple with high operational speed. Some drawback of this technique is the waste of a large amount of material, which depends on the geometry of component. Low strength because of a fragile wall (~1 mm) and anisotropy of mechanical properties [59]. The possible field of application for LOM is patternmaking for sand casting, investment casting, and ceramic processing, which indeed reduce the process steps and cycle time [60].

5.3 Stereolithography (SLA)

Stereolithography (SLA) generally known as Photopolymerization. The UV radiation or scanning laser is used to curing the photosensitive monomer resin, and the photoresin fluid is transferred into a cross-linked solid [61]. The highly detailed components having dimensions in the range of micrometer to millimeter can be easily fabricated by SLA, a specimen is shown in Fig. 7b. According to a design, the cross-section of the part is scanned by a laser beam up to a certain depth of photoresin. The accuracy of the laser beam is controlled by the motion of orthogonal revolving mirrors, after the complete scanning of the photoresin of current layer.

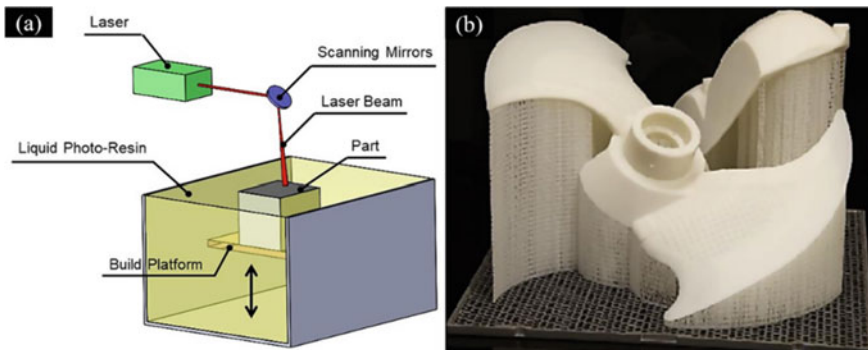


Fig. 7 a Schematic of stereolithography (SLA) adapted from Razavykia [58] b Specimen of a model fabricated by SLA method prior to the elimination of the supports [59]

The building platform moves downward, and the feed stocker recoats the part by photoresin according to required thickness as shown in Fig. 7a, the layer is scanned again [62]. For achieving the required mechanical properties, the crosslinking reaction has to be complete. Therefore, the post-processing curing process is an essential process of SLA to complete the crosslinking [63].

By controlling the viscosity and photoreactivity of photoresin we can tailor the mechanical (Young's modulus, and strength) properties of the SLA components over the wide range [64]. Moreover, the mechanical properties are highly reliant on the photopolymer network density; for example, elastomeric properties are desirable in tissue engineering and biomedical. Therefore, the photoresin with lower network density is used to achieve elastomeric properties because, by solvent, we can easily replace the large fraction of resin [65]. Some applications of SLA are dental models, fast prototypes, hearing aids, and electronic circuit printing.

5.4 Selective Laser Sintering (SLS)

Selective laser sintering is a subcategory of powder bed fusion technology that manufactures 3D layered models/components using laser beams [66]. The different binding methods such as chemical reactions, solid-state sintering, and fractional melting or complete melting methods are used in SLS to join the powder particles [67]. This method sinters the powder by heating, and this heating is generated by the laser scanning in a controlled manner, as clearly shown by the schematic in Fig. 8a. Under a high power laser, the fusion of powder occurs by molecular diffusion, and the path of laser for the selected region is controlled by the program fed to the machine. Once the layer is complete, the same process repeats for the next layer, and the same process keeps repeating until the complete component is fabricated. Finally,

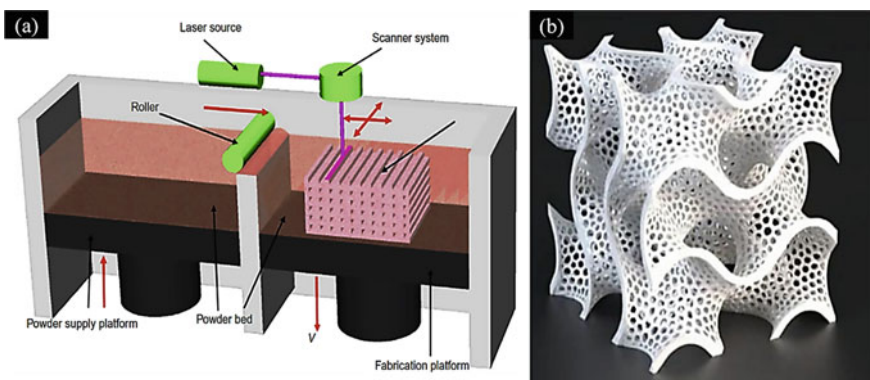


Fig. 8 a Schematic diagram of SLS 3D printing method adapted from Wang [69] b Parts made by SLS method [59]

the unused/ remaining powder is cleaned, and the final product is ready to use [68]. A complex geometry example is revealed in Fig. 8b.

The resolution/ surface finish of SLS components highly depends on the nature and size distribution of the powder particles, scanning speed, spacing, layer thickness, and laser power [70]. In the SLS process, to hold the powder particles in most cases, the liquid binder is generally used [71]. The laser sintering/binder polymer materials mostly utilize in the SLS process are polycaprolactone (PCL) and polyamide. The SLS process has some advantages, like the unused powder can be reuse (recyclability). The resolution of printing can be achieved of 20–150 μm , and an extensive series of materials can be print easily [72]. In contrast to that, having some disadvantages like the slow process compared to SLM, shrinkage in printed 3D components because of localized heating followed by rapid cooling.

5.5 Selective Laser Melting (SLM)

Selective laser melting technique comes under the Powder Bed Fusion (PBF) additive manufacturing technologies. It uses a high-intensity laser beam to melt the selective site of powder in the layer by layer manner and the path of laser decided by the computer-aided design (CAD) data. The CAD data cannot be fed directly to the SLM machine. First, we have to process the STereoLithography (STL) files using software, which prepares slice data of whole designed component for laser scanning of every layer and provide the structural support to any overhanging feature of the design, then only we can upload the CAD data to the SLM machine [73]. The process begins with putting the thin layer of metallic powder over the substrate plate inside the inert chamber. The high-power laser starts melting and fusing the metal powder from the specific area according to the program and data provided to the machine [74]. After completing the laser scanning, the new layer of metal powder (20–100 μm) was laid by the recoater by lowering the building platform with the same height of slice we prepared with STL file, and again laser will scan, shown in Fig. 9a. This

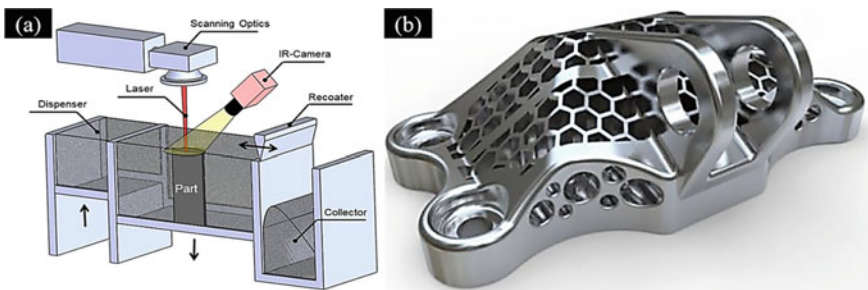


Fig. 9 a Schematic diagram of Selective laser melting (SLM) adapted from Razavykia [58] b Part made by SLM/DMLS methods [59]

process will continue automatically until the required component completely builds [75]. The remaining powder (loose powder) is cleaned from the fabrication chamber, and to separate the element from the substrate plate, we may use any manual method or electric discharge machining (EDM). Some important parameters of SLM are input power of the laser (Current and voltage), hatch spacing, scanning speed, and thickness of the layer. To prevent oxidation of the parts during fabrication, the building chamber is generally filled with inert gases like argon and nitrogen. The facility of preheating the substrate plate is also integrated with the modern SLM machine to reduce residual stresses and thermal stresses. A model fabricated by SLM is revealed in Fig. 9b.

There is no need for post-processing and post-machining in SLM except for detaching the substrate plate from the parts and supports. SLM can produce fully dense near-net-shape components because, during the process, we can achieve complete melting of the material powder. These all capabilities of SLM make it a superior AM process as compared to SLS. The SLS binds the materials powder by melt the binder agents or solid-state sintering. There is no fully melting of powders which results in low strength and porosity. Therefore post-processing is always the necessary step in SLS [73].

5.6 *Electron Beam Melting (EBM)*

Electron beam melting also belongs to the category of SLM and SLS, i.e., Powder Bed Fusion (PBF) AM technologies. However, it has some working differences and advantages over them. In EBM, the electron beam is employed to melt or fuse the metal powder in place of a laser beam, and most of the laser-based process required an atmosphere of inert gases. In contrast, the electron beam required a vacuum environment. The schematic of the EBM machine with one example of complex geometry fabricated is shown in Fig. 10a, b. The vacuum environment in EBM creates a considerable difference compared to laser-based systems because the high temperature can be achieved to fabricate parts without considering the risk of oxidation. However, the EBM system is very expensive because of the building vacuum inside the fabrication chamber. The residual stresses are also lower as compare to laser-based systems [76]. There is no need to post-processing (stress-relieving, machining) the components manufactured by the EBM [76].

The EBM preheat the powder inside the powder hopper before the melting phase, hence reduce the temperature gradients, due to which no formation of heat cracks [79]. EBM is one of the superior technology that works with a wide range of materials, including stainless steel (17-4), tool steel (H13), titanium and its alloys, Nickel alloys (IN 718, IN 625, etc.), cobalt-based alloys (Stellite 21), Invar, hard metals (NiWC), copper, niobium, and aluminium alloys along with complex geometry and fully dense components [80–82]. The SLM and SLS systems give a better surface finish than EBM because of the smaller laser beam size, and the powder thickness layer led down by the recoater is thinner [76].

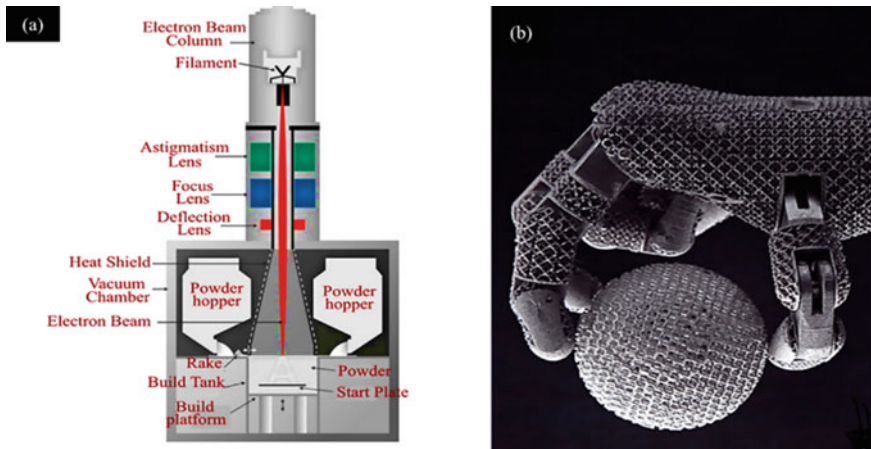


Fig. 10 a Components of an Arcam machine (an EDM machine) adapted from Galati [77], and b An example of model [78]

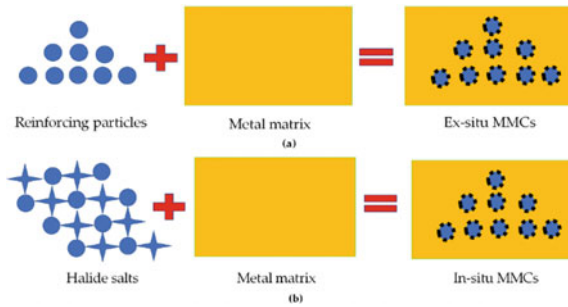
The MMCs can be manufactured by using any technique except LOM, as discussed above. Now emphasis on the development of MMCs and their types in the next section.

6 Additive Manufacturing Techniques for Developing MMCs

ISO/ASTM 52,900 has standardized the Additive manufacturing processes and categorized them into Powder bed fusion (PBF), material jetting, VAT polymerization, sheet lamination, binder jetting, and direct energy deposition (DED), etc. [46]. These are based on powder, liquid, solid-layer, i.e., state of raw materials as shown in Fig. 4. But, in this chapter, focus only on laser-based additive manufacturing processes. The laser-based Metal matrix composites mostly manufactured using powdered state raw material by reinforcing either by fibers or particulates. A few papers are found in the literature that shows trends to fabricate the laser-based MMCs from solid-state raw materials. The reason behind this may be it's difficult to achieve the complex geometry by using the solid-state raw material like in the case of the sheet-layer AM process [34, 70]. As a result, this chapter is limited to particulates reinforced MMCs. MMCs are made up of at least two materials: a distributed phase of metals, a ceramic, or a polymer embedded in a metal matrix (Parent material is always metal in case of MMCs).

Ex-situ MMCs and in-situ MMCs are two different types of MMCs [83]. Figure 11 depicts the schematics of both ex-situ and in-situ MMCs. Ex-situ MMCs are reinforced by externally synthesized reinforcing materials which pre-mixed with the

Fig. 11 The sketch of metal matrix composites **a** ex-situ **b** in-situ; adapted from Mahmood [86]



matrix material or fed into the melt pool independently during processing. In contrast, in-situ MMCs are reinforced by the reinforcing materials that are fully synthesized within the matrix by chemical reactions in the melt pool during processing. [1, 84]. However, in the ex-situ MMCs, complete powder melting is not needed, which is why sintering and binding-based processes such as Selective laser sintering (SLS), Direct metal laser sintering (DMLS), and Binder jetting are can be commonly used [85].

In the case of in-situ MMCs, however, complete powder melting is needed, and the most widely used processes are Selective Laser Melting (SLM) and Electron Beam Melting (EBM) [22]. In-situ synthesized composites have many advantages over other processes because of fine reinforced particle size, the better interface between the reinforcement and matrix, along with homogeneous distribution, due to which they have much improved mechanical properties as compared to ex-situ composites [87, 88]. Moreover, for large-scale production of in-situ MMCs, the casting route is economical and more accessible than powder metallurgy and other processes [89]. However, because of design constraints like complexity and fast analysis of parameters, laser-based AM processes are preferred. In-situ light weight Al and its alloy composites are commonly reinforced by the Mg_2Si , ZrB_2 , TiC , TiB_2 , AlN , and Al_2O_3 [4].

The LBAM is the most potential and fast way to manufacture both ex-situ and in-situ composites, which shows significantly high mechanical properties [90]. Mechanical properties are discussed in the next section by considering different studies from the literature. The energy/ enthalpy generate by the laser is effectively used to complete the reaction in in-situ reinforced MMCs. However, it has also been found that in-situ composites are thermodynamically more stable as compare to ex-situ because they form as an equilibrium product of the reaction [91]. Some reactions of In-situ reinforcement are summarized in Table 2.

Table 2 Summarizing In-situ reinforcement reactions

Reinforcements	Reactions	References
TiB ₂ and ZrB ₂	$2\text{KBF}_4 + 3\text{Al} = \text{AlB}_2 + 2\text{AlF}_3 + 2\text{KF}$ $\text{K}_2\text{TiF}_6 + 133\text{Al} = \text{TiAl}_3 + 43\text{AlF}_3 + 2\text{KF}$ $\text{K}_2\text{ZrF}_6 + 133\text{Al} = \text{ZrAl}_3 + 43\text{AlF}_3 + 2\text{KF}$ $\text{TiAl}_3 + \text{AlB}_2 = \text{TiB}_2 + 4\text{Al}$ $\text{ZrAl}_3 + \text{AlB}_2 = \text{ZrB}_2 + 4\text{Al}$	[92]
Al ₄ SiC ₄	$4\text{Al} + 3\text{SiC} = \text{Al}_4\text{C}_3 + 3\text{Si}$ $4\text{Al} + 4\text{SiC} = \text{Al}_4\text{SiC}_4 + 3\text{Si}$	[93–95]
AlN	$2\text{Al} + \text{N}_2 = 2\text{AlN}$ $2\text{Al} + 2\text{NH}_3 = 2\text{AlN} + 3\text{H}_2$	[96, 97]
Al ₂ O ₃	$\text{Fe}_2\text{O}_3 + 2\text{Al} = \text{Al}_2\text{O}_3 + 2\text{Fe}$	[98]
Al ₂ O ₃	$4\text{Al(l)} + 3\text{TiO}_2\text{(s)} = 2\text{Al}_2\text{O}_3\text{(s)} + 3\text{Ti(s)}$	[99]

7 Mechanical Properties of Lightweight MMCs Made by Additive Manufacturing as a Function of Reinforcement Features

Mechanical properties of laser-based Light weight MMCs have been broadly studied, and remarkable improvement has been recorded in both in-situ and ex-situ reinforced composites. Here are some relevant studies selected from the literature to completely understand the mechanism behind the improvement of mechanical properties.

7.1 Hardness

The effect of in-situ ZrB₂ particles on microhardness and macrohardness of AA6061 has been studied by I. Dinaharan et al. [100]. The trend of microhardness and macrohardness increases as the weight percentage of ZrB₂ increases, the changes in microstructure with varying ZrB₂ from 0 to 10% are revealed in Fig. 12 (a-h). The microhardness of AA6061- 10%ZrB₂ composite is 32.71% higher, and macrohardness is 42.65% higher concerning AA6061 alloy; the trend is shown in Fig. 12 (i). This significant improvement in the microhardness and macrohardness may be a result of ZrB₂ in the matrix. The dislocation density of composite may be increased during solidification because of ZrB₂ particles occurrence and having different coefficients of thermal expansion of reinforcing and matrix materials. Increases in the density of dislocations and the reinforcement particles, in turn, provide the resistance to the movement of dislocations on slip systems; hence plastic deformation becomes difficult. Therefore, the hardness is improved significantly.

Chang et al. [101] have shown that the microhardness of the SLM processed Aluminium matrix composites can be improved just by varying the initial size of SiC particles in the in-situ hybrid reinforced (Al₄SiC₄ + SiC) composites, as revealed in

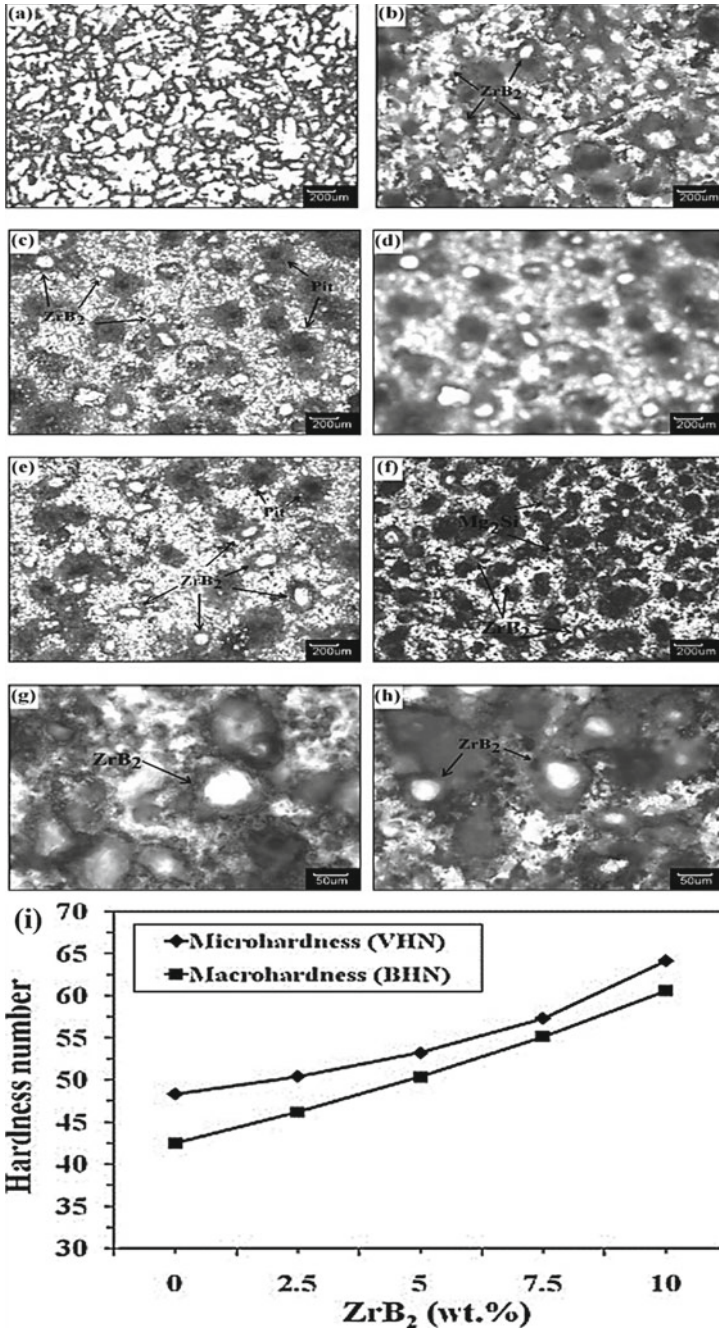


Fig. 12 Optical images of AA6061 based composite containing varying ZrB₂ reinforcement: **a** 0% ZrB₂, **b** 2.5% ZrB₂, **(c and d)** 5% ZrB₂, **e** 7.5% ZrB₂, **f** 10% ZrB₂, **g** 5% ZrB₂ and **h** 7.5% ZrB₂, **i** microhardness and macrohardness of AA6061 based composite as a function of ZrB₂ weight percentage adapted from Dinaharan [100]

Fig. 13e. Typically, the microhardness of SLM processed composites is higher due to higher cooling and heating rates related to conventional processes. However, densification and reinforcement can be the vital factors that influence the microhardness of Al matrix composites processed by SLM. In this study, the SLM processed Al matrix is reinforced by various reinforcing phases, i.e., residual/Coarse SiC particles, Al_4SiC_4 having particle and plate-like structure as clearly presented in Fig. 13a–c. The average value of microhardness of Al matrix composite reinforced by the Coarse SiC particles is 127 $HV_{0.1}$ which is even below the unreinforced SLM processed AlSi10Mg alloy (approximate maximum value 145 $HV_{0.1}$). Improper melting of SiC particles is the major cause for the fragile interfacial bonding among the Al matrix and residual SiC particles and the presence of micro pores due to which relatively lower density and hence lower microhardness as revealed in Fig. 13d, e. One more

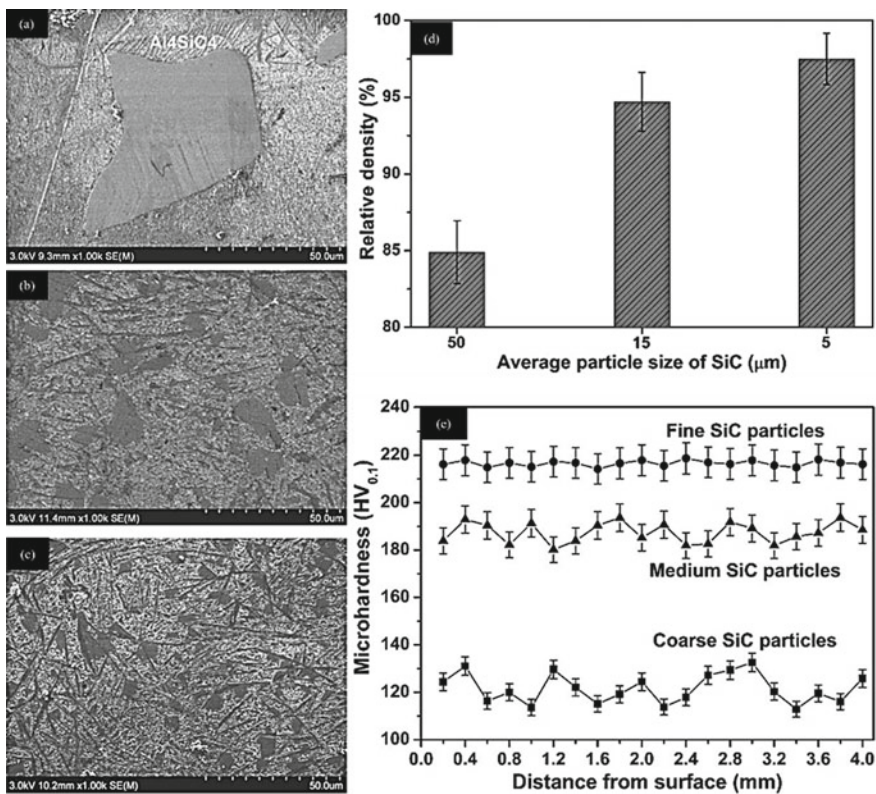


Fig. 13 FE-SEM images presenting the microstructure of SLM-processed ($Al_4SiC_4 + SiC$)/Al hybrid reinforced composites with different particle sizes of the starting SiC reinforcing powder: **a** particles of coarse SiC ($D_{50} = 50 \mu m$); **b** particles of medium SiC ($D_{50} = 15 \mu m$); and **c** particles of fine SiC ($D_{50} = 5 \mu m$) **d** relative density variation of SLM-processed ($Al_4SiC_4 + SiC$)/Al composite samples, and **e** variation in microhardness of SLM-processed ($Al_4SiC_4 + SiC$)/Al hybrid reinforced composites by varying the initial particle size of SiC adapted from Chang [101]

possibility is that the micropores or weak interface have underneath the micro indent during the test, and a considerable variation in microhardness was recorded. When the medium size SiC particles are reinforced in the Al matrix, the average microhardness was recorded is 188 HV_{0.1} along with reduced fluctuation in it, which is because of improvement in the reaction and melting of SiC particles hence higher densification, reduction in micropores, and the better interface between the reinforced SiC particles and Al matrix. The SLM processed Al matrix reinforced by the fine SiC particles had made the ultrafine particle-shaped Al₄SiC₄ reinforcement and meanwhile formed in-situ plate-like Al₄SiC₄ reinforcement, shown the remarkable improvement in the microhardness of the SLM processed aluminium based composite. The composite with fine SiC has considerably achieved the average hardness of 218.5188 HV_{0.1}. By reducing the size of SiC particle from coarse to fine, the microhardness was improved significantly because of full densification rate was achieved during the process. Since the ultrafine and plate-like structures of Al₄SiC₄ reinforcement have produced coherent interface bonding among the matrix and reinforced particles, the dispersion strengthening effect these are the main reason for improving the microhardness. Moreover, the heterogeneous nucleation sites provided by the ultrafine SiC₄ particles during solidification and the matrix's grain size are also refined. Thus the combined effect of grain refinement and dispersion strengthening comes into play in SLM processed hybrid Al matrix composites.

Dongdong Gu et al. [102] have studied the Carbon nanotube (CNTs) reinforced Al-based nanocomposites manufactured by SLM. Figure 14h depicts the microhardness of CNTs/Al-based composites at different process parameters of SLM. The optimum scanning speed was 2.0 m/s, at which maximum microhardness was achieved, i.e., 154.12 HV_{0.2}. Interestingly, at all the scanning parameters, the microhardness of SLM processed CNTs/ Al composites specimen is higher than the AlSi10Mg alloy (SLM processed) specimen, i.e., 127 ± 3 HV_{0.5} and even from the components of CNTs/Al composites specimen manufactured by the powder metallurgy (<100 HV) [103]. Microhardness distribution depends upon the densification and the microstructure formed during solidifying the components [104]. At high scanning speed, the fluctuation in microhardness was noticed because the material does not get sufficient time to solidify appropriately and achieve the optimum densification. The maximum microhardness achieved during the optimum scanning speed (2.0 m/s) is because of proper densification along with the reinforced CNTs, and the Si precipitated particles are enveloped by Al₄C₃ as shown in Fig. 14g, supporting EDX also show the elements present in the enveloped region, i.e., Al, Mg, Si, C. This Al₄C₃ has improved the interface bonding between the reinforced CNTs and matrix materials significantly, hence increased the resistance to plastic deformation [105].

At relatively higher (2.2 and 2.4 m/s) and lower (1.8 m/s) scanning speeds, much fluctuating behaviour was observed in the microhardness as compare to optimum (2 m/s) scanning speed as shown in Fig. 14h because of limited densification and lack of interface between the matrix and reinforced CNTs. However, at the optimum scanning speed, the perfect combination of densification and interface is achieved. Moreover, the grain refinement of the Al matrix, the Si particles precipitates, and

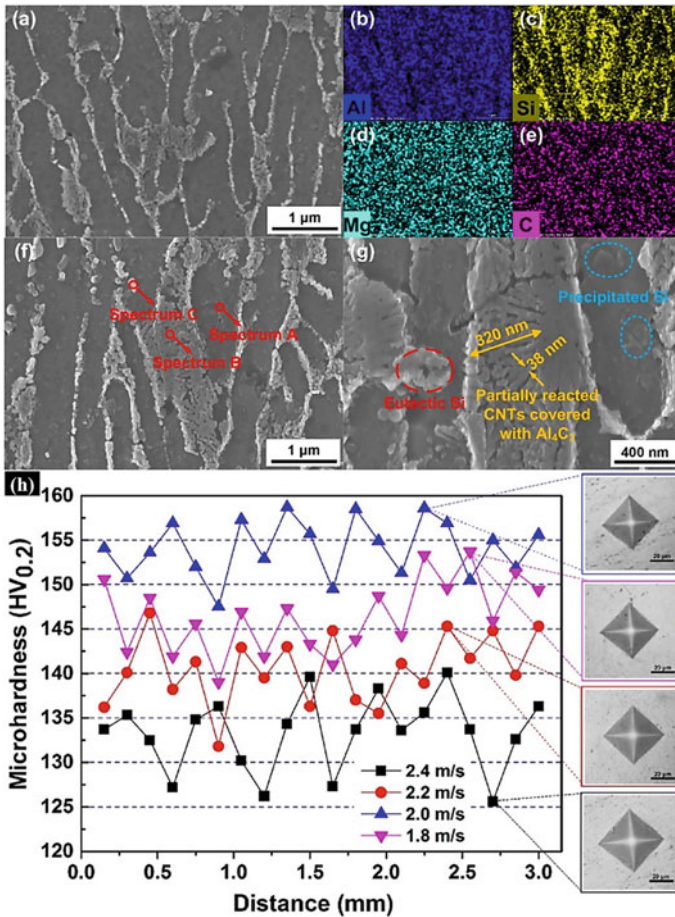


Fig. 14 a FE-SEM images of SLM-processed CNTs/Al composite samples microstructure, manufactured at Power = 350 W and scanning speed = 1.8 m/s; the elemental distributions of **b** Al, **c** Si, **d** Mg, and **e** C elements through EDX mapping; **(f, g)** SLM-processed CNTs/Al composite sample microstructures, fabricated at Power = 350 W and scanning speed = 2.0 m/s, **f** low magnification **g** higher magnification, and **h** microhardness distributions of samples processed at different SLM parameters along with indent FE-SEM images, adapted from Gu [102]

CNTs are covered by the Al₄C₃, which led to further improvement in the microhardness. The microstructure at optimum scanning speed is revealed in Fig. 14a. The Al₄C₃ has covered the outer most layer of reinforced CNTs, which have improved the interface abruptly between the Al matrix and CNTs, which further enriched the hurdle to the plastic deformation. Hence the microhardness and tensile properties improved significantly. Some of the aluminium-based composites studies are considered in the next section. The tensile and compressive strengths are broadly discussed with the

Table 3 Representing the outcome of reinforcement on the microhardness/hardness of composites

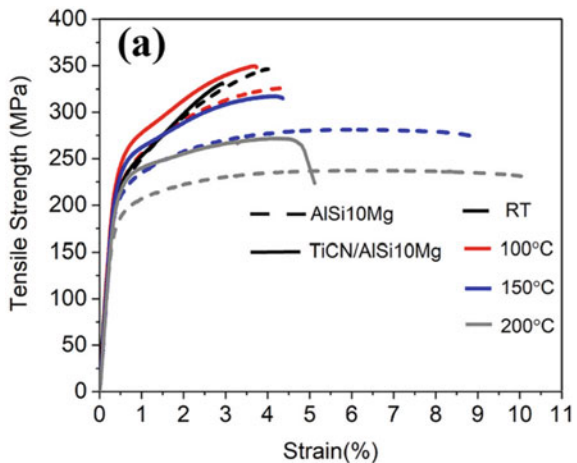
Process	Materials		Microhardness/hardness	References
	matrix	Reinforcement		
SLM	AlSi10Mg	0.5% MWCNT	Enhanced by 8.264%	[106]
SLM	AlSi10Mg	4wt%Cr ₃ C ₂ -25% NiCr	Enhanced by 32%	[107]
SLM	Ti6Al4V	Mixed gas atmosphere (N ₂ and Ar)	Enhanced by 36.3%	[108]
SLM	AlSi10Mg	Submicro-TiB ₂	Increased by 110%	[109]
Laser solid forming (LSF)	2024Al	3%TiB	Enhanced by 44.667%	[110]
SLM	AlSi10Mg	0.5 wt.% GNP	Improved by 23.95%	[111]
		1 wt.% GNP	Improved by 30.53%	
		2.5 wt.% GNP	Improved by 75.3%	

help of mechanisms responsible for the improvement. Here, some more studies on microhardness/hardness are concise in Table 3.

7.2 Tensile Strength and Compressive Strength

Peidong He et al. [112] have studied the tensile stress–strain behaviour over the temperature range (25–200 °C) of TiCN/AlSi10Mg composite and AlSi10Mg manufactured by the LPBF techniques, as shown in Fig. 15a. The TiCN/AlSi10Mg

Fig. 15 a Tensile tests curves of the LPBF TiCN/AlSi10Mg composite and AlSi10Mg alloy at different temperature ranges (RT to 200 °C) adapted from Peidong [112]



composite (333 ± 2 MPa) having the lower UTS at room temperature as compare to AlSi10Mg (356 ± 10 MPa) because of stress concentration in particles due to which the interfacial linkage between the matrix material and reinforced particles starts breaking from the weak grain boundaries, and hence premature failure occurs. However, the composite has shown a higher yield strength throughout the temperature range, including room temperature and high UTS at elevated temperatures. The micro-sized TiCN particles present at grain boundaries have formed the bridging between the grains. Moreover, they also create heterogeneous nucleation sites during solidification hence grains refinement occurs. They collectively help in strengthening the grain boundaries and improving the tensile yield strength throughout the temperature range. While, at elevated temperature, the tensile strength is reduced, but the elongation to failure improved significantly, which means higher ductility but lower tensile strength. At higher temperatures, the multi-slip systems are activated because of the mobility of atoms; hence the resistance to movement of dislocations is reduced. The elongation difference at elevated temperature may be because of the transition in the microstructure of LPBF AlSi10Mg having coarse-grained structure to bimodal structure of LPBF TiCN/AlSi10Mg. Moreover, the ductility of the LPBF TiCN/AlSi10Mg composite is less as compare to LPBF AlSi10Mg this is attributed to micro-sized TiCN particles at grain boundaries and bimodal grain structure [113]. They have created a hindrance to the movement of dislocations, hence improving tensile strength as clearly depicted in Fig. 15a.

This study shows that the LPBF TiCN/AlSi10Mg composite can be a promising candidate for high-temperature applications as compare to LPBF AlSi10Mg because it retains its ultimate strength and yield strength even at elevated temperature. In contrast, the Al matrix composites fabricated through casting have lower strength than LPBF because refined grains can be easily achieved in LPBF while we get coarse grains by casting [114]. Moreover, this TiCN ceramic particles reinforced composite (TiCN/AlSi10Mg) can be a better choice than heat-treated Al alloys because they are precipitation hardened. However, these thermally stable TiCN particles reinforced in the AlSi10Mg matrix further promote grain refinement during the LPBF process, directly supporting attaining the higher tensile strength. In addition, TiCN (Compare to SiC) has a significantly less tendency to react with the elements present in the AlSi10Mg matrix and create any brittle phase itself in the composite. Hence it's a potential reinforcement element for the AMMCs [115].

Wang et al. [116] studied the mechanical behavior of SLM processed Al0.9CoCrFeNi high-entropy alloy particles reinforced AlSi10Mg matrix composite. Three different samples of HEA/Al-10Si-Mg were manufactured using the same parameters of SLM apart from power input, i.e., 190, 220, and 250 W, and the specimens are named SLM C1, SLM C2, and SLM C3, respectively. The microstructures are shown in Fig. 16b–d along with SLM- Al-10Si-Mg (Fig. 16a). Figure 16e depicts that the maximum compressive strength and yield strength achieved by the SLM C1 specimen are 901 ± 13 MPa and 515 ± 7 MPa, respectively. The strength decreases considerably by enhancing the power input of the laser. The SLM C1 specimen of the present work reveals higher strength than other AMCs, as compiled in Fig. 16f. The weld pool temperature increases as the power input of laser increase from 190

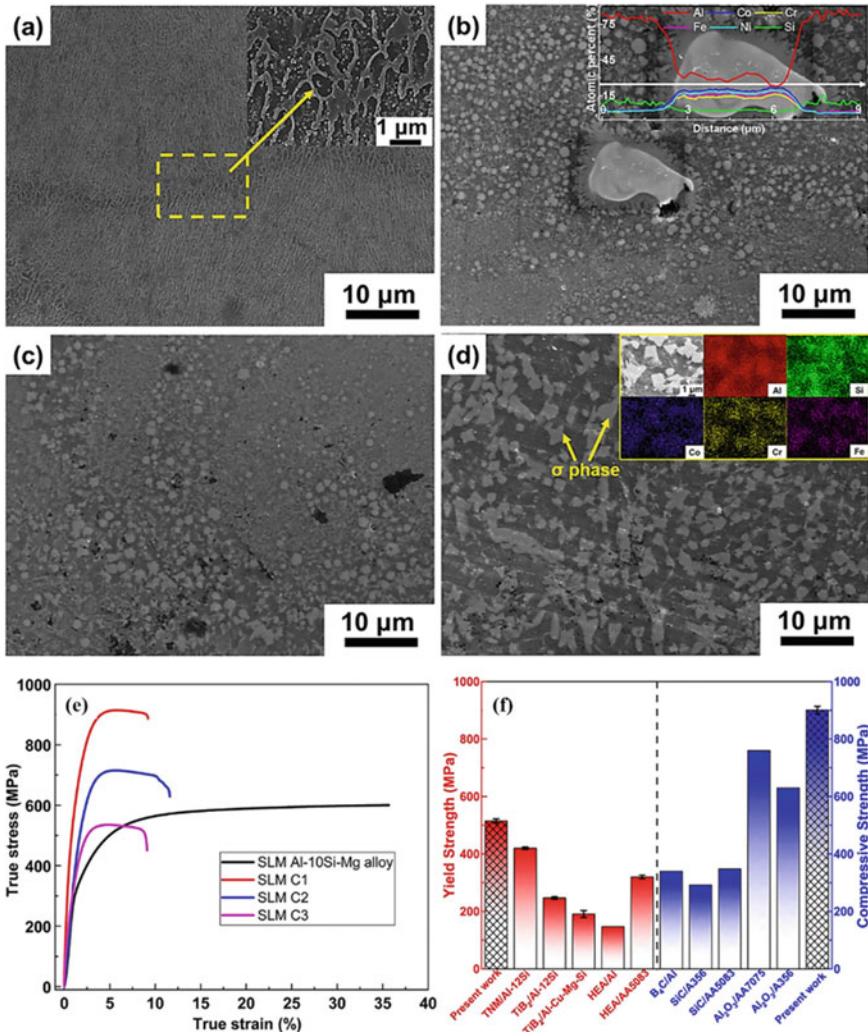


Fig. 16 SEM images of **a** SLM processed Al-10Si-Mg, with high magnification insert **b** SLM C1 (insert: EDX mapping through BCC phase), **c** SLM C2, **d** SLM C3 (insert: SEM image and corresponding EDS mapping of σ phase) **e** curve of compressive true stress-true strain for all specimens, **f** other AMCs compressive properties comparison with SLM HEA/Al-10Si-Mg adapted from Wang [116]

to 250 W as a consequence of high energy density, and hence more reaction starts occurring among the particles of HEA and the Al-10Si-Mg matrix, which accelerate the formation of Fe–Cr σ phases (brittle), the σ phases with EDS mapping is revealed in Fig. 16d [117, 118]. The σ phases hinder the formation of columnar grains of α -Al phase by serving the newly created nuclei site for crystal growth. Moreover, the

compressive strength of SLM HEA/Al-10Si-Mg composites (SLM C2 and SLM C3) reduced at higher power inputs is because of the increment in size and amount of σ phases. The SLM C1 has the residual hard HEA phases and the α -Al phase, which has a higher dislocation density. Therefore, it attains maximum compressive strength, the strength of the Al10SiMg matrix also improved because of grains of similar size [119].

Liu et al. [120] study results revealed that the SLM manufactured TiC-TiH₂/AA2024 aluminium composite shows remarkable mechanical properties. The tensile test results are presented in Fig. 17a. The tensile properties of both the as-built AA2024 (240 ± 10 MPa) specimen and TiC-TiH₂/AA2024 (390 ± 15 MPa) sample are much higher as compare to as-cast AA2024 aluminium alloy (185 MPa) [121]. Moreover the elongation percentage of as-built AA2024 specimen and TiC-TiH₂/AA2024 composite specimens are $0.3 \pm 0.2\%$, and $12.0 \pm 0.5\%$, respectively. This enhancement in mechanical properties is by virtue of grain refinement and pinning effect on the grain boundaries promoted by the TiC nanoparticles. In addition to this, the dislocation movement is hindered by a higher volume fraction of fine equiaxed grains at grain boundaries. The tensile strength and elongation percentage of SLM processed TiC-TiH₂/AA2024 composite specimen when heat treatment (T6) achieve 490 ± 20 MPa, and $16.0 \pm 1\%$, respectively, which is very near to the traditionally forged AA2024-T6 alloys [121].

Remarkably, the serrated stress-strain curve of the TiC-TiH₂/AA2024 composite specimen in Fig. 17a shows the Portevin-Le chatelier (PLC) effect. That is because of the interaction between mobile dislocations, Al₃Ti/TiC particles, and diffusing solute atoms during the tensile testing [122, 123]. Furthermore, the yield plateau also appears in SLM processed TiC-TiH₂/AA2024 composite, making it different from the wrought aluminium alloys. This appearing of yield plateau may happen because of inoculation with TiC-TiH₂ nanoparticles. However, similar changes in the tensile test curve were also stated in other aluminium alloys fabricated with SLM and having refined equiaxed grains [122, 123]. To completely understanding this mechanism, more studies are required in this field.

Tensile fracture surface micrographs are shown in Fig. 17b-e. The AA2024 sample fracture morphology revealed columnar arms, and the grain boundaries consist of a brittle fracture zone (Fig. 17b). In the case of TiC-TiH₂/AA2024 sample fracture surface, the absence of columnar fracture feature is noticed, and the dimples with fine and uniform morphology along with particles that have precipitated at the bottom of dimples were noticed, which is an indication of ductile fracture mechanism (Fig. 17c). The heat-treated (T6) AA2024 sample majorly showing brittle fracture mode. However, it also consists of some shallow dimples region mainly because of coarse columnar grains and some cracks existence between those columnar grains (Fig. 17d). While in the case of the T6 heat-treated TiC-TiH₂/AA2024 specimen, the ductile fracture features are still present. The properties are further improved because of the homogenous and uniform distribution of TiC nanoparticles and the reduction in pores (Fig. 17e). So far, additive manufacturing methods, fabrication of MMCs and their different classifications, and how the mechanical properties are improved

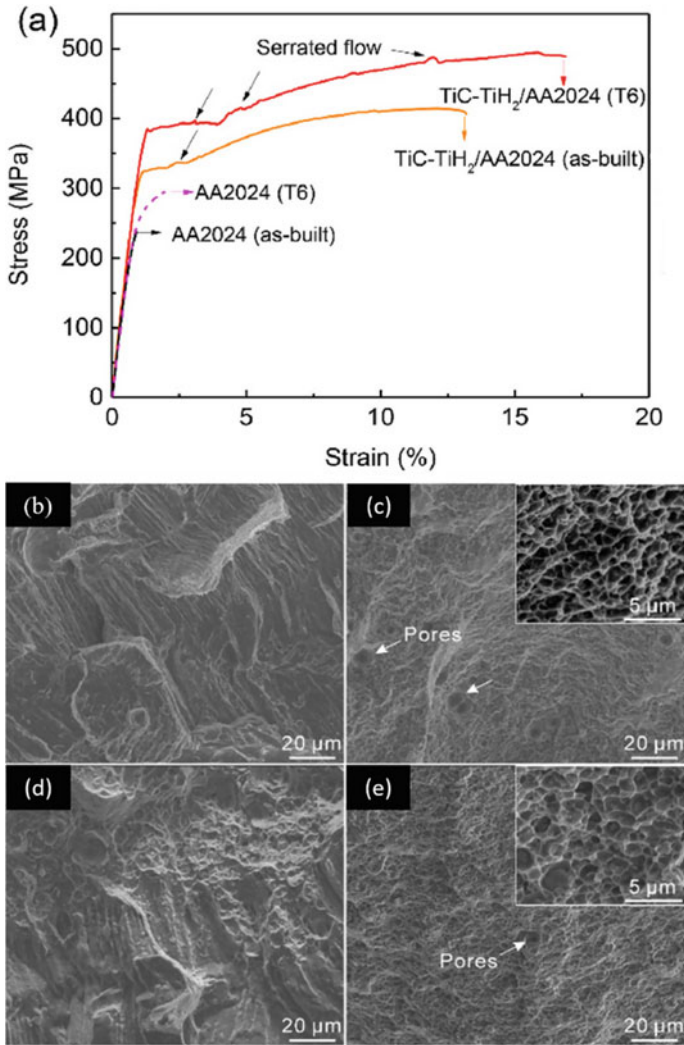


Fig. 17 a Tensile test curves of AA2024 and TiC-TiH₂/AA2024 specimens fabricated by SLM. Factographs of SLM processed b, d AA2024 specimen and c, e TiC-TiH₂/AA2024 specimen. b, c As-built, d, e after T6 heat treatment adapted from Liu [120]

being discussed, but the applications they concern about in different industrial sectors are discussed in the next section.

8 Applications of Additively Manufactured Lightweight MMCs

In contrast to conventional alloys and metals, additively manufactured lightweight MMCs are highly appreciated in applications where weight and complex design are the most important consideration. Therefore aerospace, automotive healthcare, and electronics and electrical sectors are some of the common sectors as mentioned below.

(i) Automotive sector: Nowadays, AM gets the attention of the automobile sector because of its ability to manufacture complex geometry components from small to medium size like fuel injectors, carburetors, valves, and turbocharger wheel. AM has proven that it can reduce the weight of complex components without compromising the strength, reducing operating expenses and a lower rate of fuel consumption. Complex parts of automobiles are generally manufactured by expensive casting and followed by machining process, due to which the cost of parts increases. Hence the AM is less expensive as compared to the casting process. [124]. An additively manufactured racing car upright as shown in Fig. 18a.

(ii) Electrical and electronics sector: Recently, a satellite communication antenna system was fabricated using Aluminium by additive manufacturing in a single integrated piece [129]. But the fabrication or joining of Aluminium conductors is not easy by Additive manufacturing or conventional techniques because of the low absorptivity of laser and oxidation during processing. The LPBF AlSi10Mg alloy is the only Al alloy that is most investigated based on mechanical properties

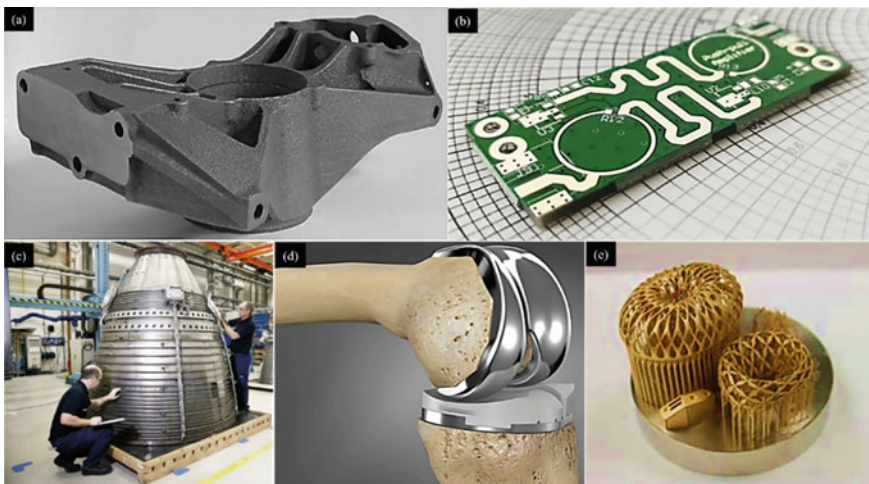


Fig. 18 a Additively manufactured, a race car upright was made adapted from Petrovic [125] b 3D Printed RF Electronics component [126]. c A model of Vulcain 2 nozzle fabricated by DED having more than 50 kg weight [115, 127] d Knee cap replacement components manufactured using 3D printing [20], and e A jewellery fabricated by AM [128]

and process parameters- microstructural correlation. However, It is found that the as-cast Al alloy having much lower resistivity as compare to LPBF AlSi10Mg, so more exploration is required to lower down the resistivity and make it a suitable material and process for electrical applications [130]. An example of an antenna component is shown in Fig. 18b. Interestingly, a study has confirmed the reduction in electrical resistivity of an additively manufactured AlSi10Mg alloy by coating it through Ag–Cu. Moreover, the Ag–Cu coating reduced the surface discontinuities like porosity, micropores. It improved the surface roughness and a noticeable improvement in the corrosion resistance of the additively manufactured AlSi10Mg alloy [131].

(iii) Aerospace sector: Lightweight composites are the most demanding material in the aerospace industry because of lightweight, but the challenges of achieving mechanical properties with the complex design requirement are not possible with conventional technologies. At present, AM is the technology that can accept all these challenges with material and cost optimization. Some most frequently used AM techniques in aerospace industries are SLM, EBM [132], SLS [133], FDM, and DED [1]. AM is the most exploring field for the fast repairing and fabrication of small volume complex aerospace parts like aircraft wings, injectors, nozzle, diffuser vanes to support space exploration [134]. “GKN Aerospace has reduced the production time and cost by approximately 30% and 40% respectively by manufacturing the 2.5 m diameter nozzle (see Fig. 18c) by additive manufacturing (DED) for ‘VULCAN 2.1’ engine manufactured by ‘AIRBUS SAFRAN LAUNCHERS’ which also reduced the around 100–1000 small components” [135]. Ding et al. have studied a thin-walled component of variable thickness manufactured by an arc welding-based AM process for an aircraft [136].

(iv) Healthcare sector: Biomedical is the major sector in which the AM is the most demanding fabrication process. It is one of the industries where the most customized and complex components are to be required. AM can quickly fabricate any complicated customized component for specific personal requirements. Nowadays, it is possible to fabricate the bones, jawbones, knee caps, windpipes, cell cultures, vascular networks, and hip joints by AM techniques. SLS, FDM, SLM, and Inkjet 3DP are some techniques for medical applications [137]. The materials commonly used for biomedical applications are composites, metals, ceramics, semi-crystalline, and amorphous thermoplastics. The examples of knee cap replacement is shown in Fig. 18d. Earlier, the surgeons have manipulated the standard casted implants themselves to make them suitable for a patient, but sometimes that is very difficult for the body to accept that implant. Therefore today, the AM gains tremendous importance in this field because of its accuracy, time-saving, and cost-effectiveness [138].

(v) Architectural and jewellery industry: The architectural and jewellery parts are highly complex in shapes that require lots of manual effort and skills that are time-consuming, costly, and sometimes even the design is so complex that it’s impossible to manufacture manually [62, 128]. Therefore this sector also started taking advantage of AM. An example of additively manufactured jewellery is shown in Fig. 18e.

The additively manufactured MMCs can be promising candidates in almost all the major sectors because they have better properties than conventionally manufactured

MMCs. Complex geometry can be easily fabricated, and the cost is also lesser. However, they have some limitations, and those limitations are pointed in the next section along with the conclusion of this chapter and the future potentials.

9 Limitations

Some contest regarding the fabrication of MMCs by AM process has been summarized as follows [7, 139–143].

1. During the additive manufacturing process, some unwanted reactions may occur between the elements present in the system, which may depreciate the composite's material characteristics, mechanical properties, and corrosive behaviour.
2. High energy input and turbulence in the melt pool may promote the uneven dissolution of elements during the AM processing.
3. Thermal stresses and residual stresses may generate cracks at the interaction of reinforcement and matrix or in the layers deposited by AM because of high solidification rate, thermal gradient between the layers, and the reinforcement and matrix material having a different coefficient of thermal expansion.
4. The high energy density input and over-heating to the system during the AM process may cause the reduction in alloying element content due to which specific material properties may be altered or lost.
5. The microstructure of a single layer may change by experiencing the thermal history of subsequent layers deposition.
6. Generally, in AM ex-situ reinforced MMCs, the micro- segregation may occur during the processing. The reinforced elements segregate inside the melt pool, due to which the AM components may not accomplish the preferred properties.
7. The improper selection of process parameters may cause the balling effect. The balling effect may influence the mechanical properties, surface roughness and densification level of the AM components.
8. The most challenging task in AM is the process parameters optimization for each specific material, their alloys, and composites.

10 Conclusion

From this study following conclusions have been derived.

- By increasing the percentage of ZrB_2 reinforcement, the higher hardness is achieved because of uniform distribution, excellent bonding, and the robust interface between the reinforced (ZrB_2) particles and aluminium alloy matrix.
- The high microhardness of 218.5 $HV_{0.1}$ has been obtained in the additively manufactured (SLM) aluminium matrix composite reinforced by the SiC particles.

- The SLM processed CNTs/Al composite has shown an improved microhardness of $154.12 \text{ HV}_{0.2}$ because of grain refinement and high densification.
- The yield strength of LPBF processed aluminium matrix composites (TiCN/AlSi10Mg) improved by breaking the micro-scale reinforced particles into submicrometer and nanometer sizes.
- The SLM processed high-entropy alloy particles reinforced aluminium matrix composites have achieved a high compressive strength of $901 \pm 13 \text{ MPa}$.
- The integration of TiC–TiH₂ nanoparticles into SLM processed AA2024 improved both tensile strength ($390 \pm 15 \text{ MPa}$) and ductility ($12.0 \pm 0.5\%$) simultaneously.

11 Future Scope

In the future, firstly, more comprehensive research on materials is required because the only very selected category of materials are available for laser-based additive manufacturing. In addition to the material, which is very demanding and challenging to process, new approaches have to be developed for processing functionally graded materials, HEAs, and bulk metallic glasses. The quality of the powder should be assured before fabrication, so some mechanism has to be developed which interacts with both research institutions and industries—secondly, lack of data for each category of materials. There should be a standard system from where industries can easily access the process parameters for a specific material and the component properties required like surface roughness, mechanical properties, etc. The post-processing data should also be collected at the same platform so that industries and laboratories can easily get the initial database and can lead to a further step in the research field of additive manufacturing of lightweight components. Finally, a multiscale simulation is required, which running iteratively and help in optimizing the perfect strategy process parameters according to orientation, strength, dimensional accuracy, and surface roughness.

References

1. Fereiduni E, Yakout M, Elbestawi M (2018) Laser-based additive manufacturing of lightweight metal matrix composites. In: Additive Manufacturing of Emerging Materials. Springer International Publishing, pp 55–109
2. Islam et al (2019) Exceptionally high fracture toughness of carbon nanotube reinforced plasma sprayed lanthanum zirconate coatings. *J Alloys Compd* 777:1133–1144. <https://doi.org/10.1016/j.jallcom.2018.11.125>
3. Aynalem GF (2020) Processing methods and mechanical properties of aluminium matrix composites. *Adv Mater Sci Eng* 2020:1–19. <https://doi.org/10.1155/2020/3765791>
4. Pramod SL, Bakshi SR, Murty BS Aluminum-based cast in situ composites: a review. *J Mater Eng Perform* <https://doi.org/10.1007/s11665-015-1424-2>

5. Karbalaei Akbari M, Baharvandi HR, Mirzaee O (2013) Fabrication of nano-sized Al₂O₃ reinforced casting aluminum composite focusing on preparation process of reinforcement powders and evaluation of its properties. *Compos Part B Eng* 55:426–432. <https://doi.org/10.1016/j.compositesb.2013.07.008>
6. Borgonovo, Yu H Nanoparticle reinforced Al casting alloys
7. Tofail SAM, Koumoulos EP, Bandyopadhyay A, Bose S, O'Donoghue L, Charitidis C (2018) Additive manufacturing: scientific and technological challenges, market uptake and opportunities. *Mater Today* 21(1): 22–37. Elsevier B.V <https://doi.org/10.1016/j.mattod.2017.07.001>
8. Chen Y, Zhang Q, Chen Z, Wang L, Yao J, Kovalenko V (2019) Study on the element segregation and Laves phase formation in the carbon nanotubes reinforced IN718 superalloy by laser cladding. *Powder Technol* 355:163–171. <https://doi.org/10.1016/j.powtec.2019.07.063>
9. Brice, Dennis N (2015) Cooling rate determination in additively manufactured aluminum alloy 2219. *Metall Mater Trans A Phys Metall Mater Sci* 46(5):2304–2308. <https://doi.org/10.1007/s11661-015-2775-x>
10. Kunovjanek M, Wankmüller C (2020) An analysis of the global additive manufacturing response to the COVID-19 pandemic. *J Manuf Technol Manage* 32(9): 75–100. Emerald Group Holdings Ltd. <https://doi.org/10.1108/JMTM-07-2020-0263>
11. Longhitano GA, Nunes GB, Candido G, da Silva JVL (2021) The role of 3D printing during COVID-19 pandemic: a review. In: *Progress in additive manufacturing*, vol 6, no 1. Springer Science and Business Media Deutschland GmbH, pp 19–37. <https://doi.org/10.1007/s40964-020-00159-x>.
12. Dhawan-1 3D printed rocket engine » 3D Printing Media Network - The Pulse of the AM Industry. <https://www.3dprintingmedia.network/skyroot-aerospace-shows-off-100-3d-printed-dhawan-1-rocket-engine/>. Accessed 05 May 2021
13. Joshi SC, Sheikh AA (2015) 3D printing in aerospace and its long-term sustainability. *Virtual Phys Prototyp* 10(4):175–185. <https://doi.org/10.1080/17452759.2015.1111519>
14. Lee K-O, Lim B, Kim D-J, Hong M, Lee K (2020) Technology trends in additively manufactured small rocket engines for launcher applications. *J Korean Soc Propuls Eng* 24(2):73–82. <https://doi.org/10.6108/kspe.2020.24.2.073>
15. Tetsui T (2002) Development of a TiAl turbocharger for passenger vehicles. *Mater Sci Eng A* 329–331:582–588. [https://doi.org/10.1016/S0921-5093\(01\)01584-2](https://doi.org/10.1016/S0921-5093(01)01584-2)
16. 3D Printing Parts for Cars | GE Additive. <https://www.ge.com/additive/additive-manufacturing/industries/automotive> (accessed May 05, 2021).
17. Beiderbeck DD, Minshall T (2018) Centre for technology management centre for technology management working paper series The impact of additive manufacturing technologies on industrial spare parts strategies the impact of additive manufacturing technologies on industrial spare parts strategies <https://doi.org/10.17863/CAM.21296>
18. Liu G et al (2020) Development of Bioimplants with 2D, 3D, and 4D additive manufacturing materials. *Engineering* 6(11): 1232–1243. Elsevier Ltd. <https://doi.org/10.1016/j.eng.2020.04.015>
19. El-Mahallawy N, Palkowski H, Breitingner HG, Klingner A, Shoeib M, Diaa A (2021) Microstructure, mechanical properties, cytotoxicity, and bio-corrosion of micro-alloyed Mg–xSn–0.04Mn alloys for biodegradable orthopaedic applications: effect of processing techniques. *J Mater Res* 1–19. <https://doi.org/10.1557/s43578-021-00172-y>
20. Ni J et al (2019) Three-dimensional printing of metals for biomedical applications. *Mater Today Bio* 3:100024. Elsevier B.V. <https://doi.org/10.1016/j.mtbio.2019.100024>
21. “3D Systems launches new VSP Hybrid maxillofacial surgical guides - 3D Printing Industry.” <https://3dprintingindustry.com/news/3d-systems-launches-new-vsp-hybrid-maxillofacial-surgical-guides-189165/>. Accessed 5 May 2021
22. Gokuldoss PK, Kolla S, Eckert J (2017) Additive manufacturing processes: selective laser melting, electron beam melting and binder jetting—selection guidelines. *Mater. (Basel)* 10(6):672. <https://doi.org/10.3390/ma10060672>

23. Pollock TM, Clarke AJ, Babu SS (2020) Design and tailoring of alloys for additive manufacturing. *Metall Mater Trans A Phys Metall Mater Sci* 51(12):6000–6019. <https://doi.org/10.1007/s11661-020-06009-3>
24. Renner P, Jha S, Chen Y, Raut A, Mehta SG, Liang H (2021) A review on corrosion and wear of additively manufactured alloys. *J Tribol* 143(5). <https://doi.org/10.1115/1.4050503>
25. Wu L et al (2020) Wear resistance of graphene nano-platelets (GNPs) reinforced AISi10Mg matrix composite prepared by SLM. *Appl Surf Sci* 503:144156. <https://doi.org/10.1016/j.apsusc.2019.144156>
26. Thasleem P, Kuriachen B, Kumar D, Ahmed A, Joy ML (2021) Effect of heat treatment and electric discharge alloying on the tribological performance of selective laser melted AISi10Mg. *J Tribol* 143(5). <https://doi.org/10.1115/1.4050897>
27. Aversa et al (2019) New aluminum alloys specifically designed for laser powder bed fusion: a review. *Mater. (Basel)* 12(7):. <https://doi.org/10.3390/ma12071007>
28. Hyer H et al (2021) Composition-dependent solidification cracking of aluminum-silicon alloys during laser powder bed fusion. *Acta Mater* 208:116698. <https://doi.org/10.1016/j.actamat.2021.116698>
29. Hull W, Arcadia C (1984) United states patent (19) hull (54) (75) (73) 21) 22 (51) 52) (58) (56) apparatus for production of three-dimensional objects by stereo ethnography
30. “United States Patent (19) Crump (54) Apparatus and method for creating three-dimensional objects (1989)
31. Wohlers T, Gornet T (2014) History of additive manufacturing 2014. *Wohlers Rep 2014—3D Print Addit Manuf State Ind*, pp 1–34
32. Liu S, Shin YC (2019) Additive manufacturing of Ti6Al4V alloy: a review. *Mater Des* 164:107552. <https://doi.org/10.1016/j.matdes.2018.107552>
33. Oliveira JP, LaLonde AD, Ma J (2020) Processing parameters in laser powder bed fusion metal additive manufacturing. *Mater Des* 193:108762. <https://doi.org/10.1016/j.matdes.2020.108762>
34. DebRoy T et al (2018) Additive manufacturing of metallic components—process, structure and properties. *Prog Mater Sci* 92:112–224 Elsevier Ltd. <https://doi.org/10.1016/j.pmatsci.2017.10.001>
35. Kumar S (2014) Selective laser sintering/melting. In: *Comprehensive materials processing*, vol 10, Elsevier Ltd. pp 93–134
36. Li Y, Založnik M, Zollinger J, Dembinski L, Mathieu A (2021) Effects of the powder, laser parameters and surface conditions on the molten pool formation in the selective laser melting of IN718. *J Mater Process Technol* 289. <https://doi.org/10.1016/j.jmatprotec.2020.116930>
37. Glardon R, Karapatis N, Romano V (2001) Influence of Nd: YAG parameters on the selective laser sintering of metallic powders. *CIRP Ann Manuf Technol* 50(1):133–136. [https://doi.org/10.1016/S0007-8506\(07\)62088-5](https://doi.org/10.1016/S0007-8506(07)62088-5)
38. Zhang H LeBlanc S (2018) Processing parameters for selective laser sintering or melting of oxide ceramics. In: *Additive manufacturing of high-performance metals and alloys—modeling and optimization*, InTech
39. Levy GN, Schindel R, Kruth JP (2003) Rapid manufacturing and rapid tooling with layer manufacturing (LM) technologies, state of the art and future perspectives. *CIRP Ann Manuf Technol* 52(2):589–609. [https://doi.org/10.1016/S0007-8506\(07\)60206-6](https://doi.org/10.1016/S0007-8506(07)60206-6)
40. Rombouts M, Kruth JP, Froyen L, Mercelis P (2006) Fundamentals of selective laser melting of alloyed steel powders. *CIRP Ann Manuf Technol* 55(1):187–192. [https://doi.org/10.1016/S0007-8506\(07\)60395-3](https://doi.org/10.1016/S0007-8506(07)60395-3)
41. Li R, Liu J, Shi Y, Wang L, Jiang W (2012) Balling behavior of stainless steel and nickel powder during selective laser melting process. *Int J Adv Manuf Technol* 59(9–12):1025–1035. <https://doi.org/10.1007/s00170-011-3566-1>
42. Kruth JP, Kumar S (2005) Statistical analysis of experimental parameters in selective laser sintering. *Adv Eng Mater* 7(8):750–755. <https://doi.org/10.1002/adem.200500030>
43. Yang Y, Loh HT, Fuh JYH, Wang YG (2002) Equidistant path generation for improving scanning efficiency in layered manufacturing. *Rapid Prototyp J* 8(1):30–37. <https://doi.org/10.1108/13552540210413284>

44. Shi Y, Zhang W, Cheng Y, Huang S (2007) Compound scan mode developed from subarea and contour scan mode for selective laser sintering. *Int J Mach Tools Manuf* 47(6):873–883. <https://doi.org/10.1016/j.ijmachtools.2006.08.013>
45. Kruth JP, Kumar S, Van Vaerenbergh J (2005) Study of laser-sinterability of ferro-based powders. *Rapid Prototyp. J.* 11(5):287–292. <https://doi.org/10.1108/13552540510623594>
46. ISO/ASTM52900-15 Standard terminology for additive manufacturing—general principles—terminology. <https://www.astm.org/Standards/ISOASTM52900.htm>. Accessed May 01, 2021
47. Thompson SM, Bian L, Shamsaei N, Yadollahi A (2015) An overview of direct laser deposition for additive manufacturing; Part I: Transport phenomena, modeling and diagnostics. *Additive Manufacturing*, vol 8. Elsevier B.V., pp 36–62 (2015). <https://doi.org/10.1016/j.addma.2015.07.001>
48. Senthilkumar V, VC., Balasubramanian KR, Kumaran M (2020) Additive manufacturing of multi-material and composite parts. pp 127–146. <https://doi.org/10.4018/978-1-7998-4054-1.ch007>
49. Pratheesh Kumar S, Elangovan S, Mohanraj R, Ramakrishna JR (2021) Review on the evolution and technology of state-of-the-art metal additive manufacturing processes. *Mater Today Proc* <https://doi.org/10.1016/j.matpr.2021.02.567>
50. Udroui R (2012) Powder bed additive manufacturing systems and. *Acad J Manuf Eng* 10(4):122–129
51. Heralić, Heralić H (2012) Thesis for the degree of doctor of philosophy Monitoring and Control of Robotized Laser Metal-Wire Deposition
52. Miranda RM, Lopes G, Quintino L, Rodrigues JP, Williams S (2008) Rapid prototyping with high power fiber lasers. *Mater Des* 29(10):2072–2075. <https://doi.org/10.1016/j.matdes.2008.03.030>
53. Nie Z et al (2016) Experimental study and modeling of H13 steel deposition using laser hot-wire additive manufacturing. *J Mater Process Technol* 235:171–186. <https://doi.org/10.1016/j.jmatprotec.2016.04.006>
54. Liu Q, Wang Y, Zheng H, Tang K, Li H, Gong S (2016) Wire feeding based laser additive manufacturing TC17 titanium alloy. *Mater Technol* 31(2):108–114. <https://doi.org/10.1179/1753555715Y.0000000075>
55. Mortello M, Casalino G (2021) Transfer mode effects on Ti6Al4V wall building in wire laser additive manufacturing. *Manuf Lett* 28:17–20. <https://doi.org/10.1016/j.mfglet.2021.03.001>
56. Chlebus, Krot K (2016) CAD 3D models decomposition in manufacturing processes. *Arch Civ Mech Eng* 16(1):20–29. <https://doi.org/10.1016/j.acme.2015.09.008>
57. Hanser G, Hanser M, Understanding additive manufacturing rapid prototyping · rapid tooling · rapid manufacturing
58. Razavykia E, Delprete C Yavari R (2020) An overview of additive manufacturing technologies—a review to technical synthesis in numerical study of selective laser melting. *Mater. (Basel)* 13(17):3895. <https://doi.org/10.3390/ma13173895>
59. Gapinski PJ, Marciniak-Podsadna L, Jakubowicz M (2016) Application of the computed tomography to control parts made on additive manufacturing process. *Procedia Eng* 149:105–121 <https://doi.org/10.1016/j.proeng.2016.06.645>
60. Mueller, Kochan D (1999) Laminated object manufacturing for rapid tooling and pattern-making in foundry industry. *Comput Ind* (39)(1):47–53 (1999). [https://doi.org/10.1016/S0166-3615\(98\)00127-4](https://doi.org/10.1016/S0166-3615(98)00127-4)
61. Lee H, Lim CHJ, Low MJ, Tham N, Murukeshan VM, Kim YJ (2017) Lasers in additive manufacturing: a review. *Int J Prec Eng Manuf—Green Technol* 4(3):307–322 (2017). Korean Society for Precision Engineering. <https://doi.org/10.1007/s40684-017-0037-7>
62. Wong KV, Hernandez A (2012) A review of additive manufacturing. *ISRN Mech Eng* 2012:1–10. <https://doi.org/10.5402/2012/208760>
63. Kim H, Choi JW, Wicker R (2010) Scheduling and process planning for multiple material stereolithography. *Rapid Prototyp J* 16(4):232–240. <https://doi.org/10.1108/13552541011049243>

64. Stampfl J et al (2008) Photopolymers with tunable mechanical properties processed by laser-based high-resolution stereolithography. *J Micromechanics Microengineering* 18(12):2008. <https://doi.org/10.1088/0960-1317/18/12/125014>
65. Yu LMY, Leipzig ND, Shoichet MS (2008) Promoting neuron adhesion and growth. *Mater Today* 11(5):36–43. [https://doi.org/10.1016/S1369-7021\(08\)70088-9](https://doi.org/10.1016/S1369-7021(08)70088-9)
66. Li N, Li Y, Liu S (2016) Rapid prototyping of continuous carbon fiber reinforced polylactic acid composites by 3D printing. *J Mater Process Technol* 238:218–225. <https://doi.org/10.1016/j.jmatprotec.2016.07.025>
67. Kruth JP, Mercelis P, Van Vaerenbergh J, Froyen L, Rombouts M (2005) Binding mechanisms in selective laser sintering and selective laser melting. *Rapid Prototyp J* 11(1):26–36. <https://doi.org/10.1108/13552540510573365>
68. Gu D, Meiners W, Wissenbach K, Poprawe R (2012) Laser additive manufacturing of metallic components: Materials, processes and mechanisms. *Int Mater Rev* 57(3):133–164. <https://doi.org/10.1179/1743280411Y.0000000014>
69. Wang X, Jiang M, Zhou Z, Gou J, Hui D (2017) 3D printing of polymer matrix composites: A review and prospective. *Compos Part B: Eng* 110:442–458 Elsevier Ltd. <https://doi.org/10.1016/j.compositesb.2016.11.034>
70. Sames WJ, List FA, Pannala S, Dehoff RR, Babu SS (2016) The metallurgy and processing science of metal additive manufacturing. *Int Mater Rev* 61(5):315–360. Taylor and Francis Ltd. <https://doi.org/10.1080/09506608.2015.1116649>
71. Chiappone et al (2016) 3D printed PEG-based hybrid nanocomposites obtained by Sol-Gel technique. *ACS Appl Mater Interfaces* 8(8):5627–5633. <https://doi.org/10.1021/acsami.5b12578>
72. Kruth JP, Van Den Broucke B, van Vaerenbergh J, Van Vaerenbergh J, Naert I (2005) Digital manufacturing of biocompatible metal frameworks for complex dental prostheses by means of SLS/SLM. Taylor & Francis/Balkema publishers, Sep. 2005. Accessed 1 May 2021. [Online]. Available: <https://research.utwente.nl/en/publications/digital-manufacturing-of-bio-compatible-metal-frameworks-for-compl>
73. Yap Y et al (2015) Review of selective laser melting: Materials and applications. *Appl Phys Rev Am Inst Phys Inc* 2(4):041101 (2015). <https://doi.org/10.1063/1.4935926>
74. Clare T, Chalker PR, Davies S, Sutcliffe CJ, Tsopanos S (2008) Selective laser melting of high aspect ratio 3D nickel-titanium structures two way trained for MEMS applications. *Int J Mech Mater Des* 4(2):181–187. <https://doi.org/10.1007/s10999-007-9032-4>
75. Chua K, Leong KF (2014) 3D Printing and additive manufacturing: Principles and applications (with companion media pack) - fourth edition of rapid prototyping. World Scientific Publishing Co.
76. Froes H, Dutta B (2014) The additive manufacturing (AM) of titanium alloys. *Adv Mater Res* 1019:19–25. <https://doi.org/10.4028/www.scientific.net/AMR.1019.19>
77. Galati M, Iuliano L (2018) A literature review of powder-based electron beam melting focusing on numerical simulations. *Add Manuf* 19:1–20. <https://doi.org/10.1016/j.addma.2017.11.001>
78. “EBM (Electron Beam Melting) | LLC Fitnik technologies.” <http://fitnik.tech/en/technologies/ebm>. Accessed 02 May 2021
79. Murr LE et al (2012) Metal Fabrication by additive manufacturing using laser and electron beam melting technologies. *J Mater Sci Technol* 28(1):1–14. [https://doi.org/10.1016/S1005-0302\(12\)60016-4](https://doi.org/10.1016/S1005-0302(12)60016-4)
80. Murr LE et al (2011) Microstructural architecture, microstructures, and mechanical properties for a nickel-base superalloy fabricated by electron beam melting. *Metall Mater Trans A* 42(11):3491–3508. <https://doi.org/10.1007/s11661-011-0748-2>
81. Biamino S et al (2011) Electron beam melting of Ti-48Al-2Cr-2Nb alloy: microstructure and mechanical properties investigation. *Intermetallics* 19(6):776–781. <https://doi.org/10.1016/j.intermet.2010.11.017>
82. Fager S, Karlsson FJ, Wedel MK γ -Titanium aluminide manufactured by electron beam melting an investigation of microstructural behavior and related mechanical properties for aerospace applications diploma work in the master programme advanced engineering material

83. Yakout M, Elbestawi MA (2021) Additive manufacturing of composite materials : an overview. In: 6th International Conference Virtual Machine Process Technologies (VMPT), Montréal, no. May, pp. 1–8, 2017, Accessed: May 01, 2021. [Online]. Available: https://www.researchgate.net/publication/316688880_Additive_Manufacturing_of_Composite_Materials_An_Overview
84. Tjong SC, Ma ZY (2000) Microstructural and mechanical characteristics of in situ metal matrix composites. *Mater Sci Eng R Rep* 29(3):49–113. [https://doi.org/10.1016/S0927-796X\(00\)00024-3](https://doi.org/10.1016/S0927-796X(00)00024-3)
85. AlMangour DG, Yang JM (2017) In-situ formation of novel TiC-particle-reinforced 316L stainless steel bulk-form composites by selective laser melting. *J Alloys Compd* 706(409–418). <https://doi.org/10.1016/j.jallcom.2017.01.149>
86. Mahmood MA, Popescu AC, Mihailescu IN (2020) Metal matrix composites synthesized by laser-melting deposition: a review. *Mater (Basel)* 13(11):2593. <https://doi.org/10.3390/ma13112593>
87. Tjong SC (2007) Novel nanoparticle-reinforced metal matrix composites with enhanced mechanical properties. *Adv Eng Mater* 9(8):639–652. <https://doi.org/10.1002/adem.200700106>
88. Wang HY, Jiang QC, Li XL, Wang JG (2003) In situ synthesis of TiC/Mg composites in molten magnesium. *Scr Mater* 48(9):1349–1354. [https://doi.org/10.1016/S1359-6462\(03\)00014-9](https://doi.org/10.1016/S1359-6462(03)00014-9)
89. Ramanathan P, Krishnan K, Muraliraja R (2019) A review on the production of metal matrix composites through stir casting—furnace design, properties, challenges, and research opportunities *J Manuf Proc* 42.:213–245 (2019). <https://doi.org/10.1016/j.jmapro.2019.04.017>
90. Gu HW Zhang G Selective laser melting additive manufacturing of Ti-Based nanocomposites: the role of nanopowder <https://doi.org/10.1007/s11661-013-1968-4>
91. Gautam, Mohan A (2015) Effect of ZrB₂ particles on the microstructure and mechanical properties of hybrid (ZrB₂ + Al₃Zr)/AA5052 insitu composites *J Alloys Compd* 649:174–183. <https://doi.org/10.1016/j.jallcom.2015.07.096>
92. Zhao XL, Liu Y, Bian X In-situ preparation of Al matrix composites reinforced by TiB₂ particles and sub-micron ZrB₂
93. Shi J, Wang Y Development of metal matrix composites by laser-assisted additive manufacturing technologies: a review <https://doi.org/10.1007/s10853-020-04730-3>
94. Simchi, Godlinski D Densification and microstructural evolution during laser sintering of A356/SiC composite powders. <https://doi.org/10.1007/s10853-010-4943-0>.
95. Anandkumar R, Almeida A, Colaço R, Vilar R, Ocelik V, Th De Hosson JM (2007) Microstructure and wear studies of laser clad Al-Si/SiC (p) composite coatings <https://doi.org/10.1016/j.surfcoat.2007.04.003>
96. Cintas J, Cuevas FG, Montes JM, Herrera EJ (2005) High-strength PM aluminium by milling in ammonia gas and sintering. *Scr Mater* 53(10):1165–1170. <https://doi.org/10.1016/j.scriptamat.2005.07.019>
97. Hou Q, Mutharasan R, Koczak M (2021) Feasibility of aluminium nitride formation in aluminum alloys *Mater Sci Eng A* 195:121–129. Accessed: Apr. 30, 2021. [Online]. Available: https://www.academia.edu/6325411/Feasibility_of_aluminium_nitride_formation_in_aluminium_alloys
98. Metal process engineering/ [by] P. Polukhin [and others] ; under the editorship of P. Polukhin. Tra... | National Library of Australia.” <https://catalogue.nla.gov.au/Record/2220757>. Accessed 1 May 2021
99. Feng F, Froyen L (1997) In-situ synthesis of Al₂O₃ and TiB₂ particulate mixture reinforced aluminium matrix composites. *Scr Mater* 36(4):467–473. [https://doi.org/10.1016/S1359-6462\(96\)00387-9](https://doi.org/10.1016/S1359-6462(96)00387-9)
100. Dinaharan NM, Parameswaran S (2011) Influence of in situ formed ZrB₂ particles on microstructure and mechanical properties of AA6061 metal matrix composites. *Mater Sci Eng A* 528(18):5733–5740. <https://doi.org/10.1016/j.msea.2011.04.033>

101. Chang DG, Dai D, Yuan P (2015) Selective laser melting of in-situ $\text{Al}_4\text{SiC}_4 + \text{SiC}$ hybrid reinforced Al matrix composites: influence of starting SiC particle size. *Surf Coatings Technol* 272:15–24. <https://doi.org/10.1016/j.surfcoat.2015.04.029>
102. Gu XR, Dai D, Ma C, Xi L, Lin K (2019) Laser additive manufacturing of carbon nanotubes (CNTs) reinforced aluminum matrix nanocomposites: processing optimization, microstructure evolution and mechanical properties. <https://doi.org/10.1016/j.addma.2019.100801>
103. Thijs L, Kempen K, Kruth JP, Van Humbeeck J (2013) Fine-structured aluminium products with controllable texture by selective laser melting of pre-alloyed AlSi10Mg powder. *Acta Mater* 61(5):1809–1819. <https://doi.org/10.1016/j.actamat.2012.11.052>
104. Li JK, He C, Zhao N, Liang C, Li B (2013) Mechanical properties and interfacial analysis of aluminum matrix composites reinforced by carbon nanotubes with diverse structures. *Mater Sci Eng A* 577:120–124. <https://doi.org/10.1016/j.msea.2013.04.035>
105. Liu X et al (2018) Effectively reinforced load transfer and fracture elongation by forming Al_4C_3 for in-situ synthesizing carbon nanotube reinforced Al matrix composites. *Mater Sci Eng A* 718:182–189. <https://doi.org/10.1016/j.msea.2018.01.065>
106. Yu T, Liu J, He Y, Tian J, Chen M, Wang Y (2020) Microstructure and wear characterization of carbon nanotubes (CNTs) reinforced aluminum matrix nanocomposites manufactured using selective laser melting. *Wear* 203581. <https://doi.org/10.1016/j.wear.2020.203581>
107. Liao WZ, Chen C, Chen B, Xue G, Zhu H (2021) Hybrid reinforced aluminum matrix composites fabricated by selective laser melting. *Intermetallics* 131:107080. <https://doi.org/10.1016/j.intermet.2020.107080>
108. Wei W, Wu W, Fan S, Duan X (2021) In-situ laser additive manufacturing of Ti6Al4V matrix composites by gas–liquid reaction in dilute nitrogen gas atmospheres. *Mater Des* 202:109578. <https://doi.org/10.1016/j.matdes.2021.109578>
109. Xi L, Guo S, Gu D, Guo M, Lin K (2020) Microstructure development, tribological property and underlying mechanism of laser additive manufactured submicro-TiB₂ reinforced Al-based composites. *J Alloys Compd* 819:152980. <https://doi.org/10.1016/j.jallcom.2019.152980>
110. Wen X et al (2019) Laser solid forming additive manufacturing TiB₂ reinforced 2024Al composite: Microstructure and mechanical properties. *Mater Sci Eng A* 745:319–325. <https://doi.org/10.1016/j.msea.2018.12.072>
111. Hu Z et al (2018) 3D printing graphene-aluminum nanocomposites. *J Alloys Compd* 746:269–276. <https://doi.org/10.1016/j.jallcom.2018.02.272>
112. He P, Kong H, Liu Q, Ferry M, Kruzic JJ, Li X (2021) Elevated temperature mechanical properties of TiCN reinforced AlSi10Mg fabricated by laser powder bed fusion additive manufacturing. *Mater Sci Eng A* 811:141025. <https://doi.org/10.1016/j.msea.2021.141025>
113. Fan J, Choo H, Liaw PK, Lavernia EJ (2006) Plastic deformation and fracture of ultrafine-grained Al-Mg alloys with a bimodal grain size distribution. <https://doi.org/10.1016/j.actamat.2005.11.044>
114. Han WZ, Zhang G, Feng Z, Wang Y (2015) High-temperature mechanical properties and fracture mechanisms of Al-Si piston alloy reinforced with in situ TiB₀ particles. *Mater Sci Eng A* 633:161–168. <https://doi.org/10.1016/j.msea.2015.03.021>
115. Kori SA, Murty BS, Chakraborty M (2021) Development of an efficient grain refiner for Al-7Si alloy. Accessed: 30 Apr 2021 [Online]. Available: www.elsevier.com/locate/msea
116. Wang P et al (2021) Microstructure and mechanical properties of novel high-entropy alloy particle reinforced aluminum matrix composites fabricated by selective laser melting. *J Alloys Compounds* 868:159197 (2021). <https://doi.org/10.1016/j.jallcom.2021.159197>
117. Manzoni M et al (2016) On the path to optimizing the Al-Co-Cr-Cu-Fe-Ni-Ti high entropy alloy family for high temperature applications. <https://doi.org/10.3390/e18040104>
118. Wang WR, Wang WL, Yeh JW (2014) Phases, microstructure and mechanical properties of Al_xCoCrFeNi high-entropy alloys at elevated temperatures. *J Alloys Compd* 589:143–152. <https://doi.org/10.1016/j.jallcom.2013.11.084>
119. Wang P, Gammer C, Brenne F, Niendorf T, Eckert J, Scudino S (2018) A heat treatable TiB₂/Al-3.5Cu-1.5Mg-1Si composite fabricated by selective laser melting: Microstructure,

- heat treatment and mechanical properties. *Compos Part B Eng* 147:162–168. <https://doi.org/10.1016/j.compositesb.2018.04.026>
120. Liu X, Liu Y, Zhou Z, Wang K, Zhan Q, Xiao X (2021) Grain refinement and crack inhibition of selective laser melted AA2024 aluminum alloy via inoculation with TiC–TiH₂. *Mater Sci Eng A* 813:141171. <https://doi.org/10.1016/j.msea.2021.141171>
 121. Zhang HZ, Qi T, Hu Z, Zeng X (2016) Selective laser melting of high strength Al-Cu-Mg alloys: processing, microstructure and mechanical properties. *Mater Sci Eng A* 656:47–54. <https://doi.org/10.1016/j.msea.2015.12.101>.
 122. Tan Q et al (2020) Inoculation treatment of an additively manufactured 2024 aluminium alloy with titanium nanoparticles. *Acta Mater* 196:1–16. <https://doi.org/10.1016/j.actamat.2020.06.026>
 123. Nie X, Zhang H, Zhu H, Hu Z, Qi Y, Zeng X (2019) On the role of Zr content into Portevin-Le Chatelier (PLC) effect of selective laser melted high strength Al-Cu-Mg-Mn alloy. *Mater Lett* 248:5–7. <https://doi.org/10.1016/j.matlet.2019.03.112>
 124. Cooper JT, Blundell N, Henrys R, Williams MA, Gibbons G (2015) Design and manufacture of high performance hollow engine valves by additive layer manufacturing. *Mater Des* 69:44–55. <https://doi.org/10.1016/j.matdes.2014.11.017>
 125. Petrovic V, Vicente Haro Gonzalez J, Jordá Ferrando O, Delgado Gordillo J, Ramón Blasco Puchades J, Portolés Griñan L (2011) Additive layered manufacturing: sectors of industrial application shown through case studies. *Int J Prod Res* 49(4):1061–1079. <https://doi.org/10.1080/00207540903479786>
 126. Practical 3D Printing of Antennas and RF Electronics—Aerospace & Defense Technology. <https://www.aerodefensetech.com/component/content/article/adt/features/articles/37095>. Accessed 01 May 2021.
 127. “GKN.” <https://www.gkn.com/en/our-technology/2016/additive-manufacturing/>. Accessed 01 May 2021
 128. Cooper (2016) Sintering and additive manufacturing: ‘additive manufacturing and the new paradigm for the jewellery manufacturer’. *Prog Addit Manuf* 1(1–2):29–43. <https://doi.org/10.1007/s40964-015-0003-2>
 129. US9742069B1 - Integrated single-piece antenna feed—Google Patents. <https://patents.google.com/patent/US9742069B1/en>. Accessed 01 May 2021
 130. Silbernagel IA, Dickens P, Galea M (2018) Electrical resistivity of additively manufactured AlSi10Mg for use in electric motors. *Addit Manuf* 21:395–403. <https://doi.org/10.1016/j.addma.2018.03.027>
 131. Rautio T, Hamada A, Kumpula J, Järvenpää A, Allam T (2020) Enhancement of electrical conductivity and corrosion resistance by silver shell-copper core coating of additively manufactured AlSi10Mg alloy. *Surf Coatings Technol* 403. <https://doi.org/10.1016/j.surfcoat.2020.126426>
 132. Michaleris P (2014) Modeling metal deposition in heat transfer analyses of additive manufacturing processes. *Finite Elem Anal Des* 86:51–60. <https://doi.org/10.1016/j.finel.2014.04.003>
 133. Evers, Dotchev K (2010) Technology review for mass customisation using rapid manufacturing. *Assem Autom* 30(1):39–46. <https://doi.org/10.1108/01445151011016055>
 134. Mohd Yusuf S, Cutler S, Gao N (2019) Review: the impact of metal additive manufacturing on the aerospace industry. *Metals (Basel)* 9(12):1286. <https://doi.org/10.3390/met9121286>
 135. “GKN.” <https://www.gkn.com/en/newsroom/news-releases/aerospace/2017/gkn-delivers-revolutionary-ariane-6-nozzle-to-airbus-safran-launchers/>. Accessed 01 May 2021
 136. Ding et al (2016) Towards an automated robotic arc-welding-based additive manufacturing system from CAD to finished part. *CAD Comput Aided Des* 73:66–75. <https://doi.org/10.1016/j.cad.2015.12.003>
 137. Cui X, Boland T, D’Lima DD, Lotz MK (2012) Thermal inkjet printing in tissue engineering and regenerative medicine. *Recent Pat Drug Deliv Formul* 6(2):149–155. <https://doi.org/10.2174/187221112800672949>

138. Banks (2013) Adding value in additive manufacturing: Researchers in the United Kingdom and Europe look to 3D printing for customization. *IEEE Pulse* 4(6):22–26. <https://doi.org/10.1109/MPUL.2013.2279617>
139. Yakout M, Cadamuro A, Elbestawi MA, Veldhuis SC (2017) The selection of process parameters in additive manufacturing for aerospace alloys. *Int J Adv Manuf Technol* 92(5–8):2081–2098. <https://doi.org/10.1007/s00170-017-0280-7>
140. Ghosh SK, Saha P, Kishore S (2010) Influence of size and volume fraction of SiC particulates on properties of ex situ reinforced Al-4.5Cu-3Mg metal matrix composite prepared by direct metal laser sintering process. *Mater Sci Eng A* 527(18–19):4694–4701. <https://doi.org/10.1016/j.msea.2010.03.108>
141. Ghosh SK, Saha P (2011) Crack and wear behavior of SiC particulate reinforced aluminium based metal matrix composite fabricated by direct metal laser sintering process. *Mater Des* 32(1):139–145. <https://doi.org/10.1016/j.matdes.2010.06.020>
142. Gård PK, Bergström J (2006) Microstructural characterization and wear behavior of (Fe,Ni)-TiC MMC prepared by DMLS. *J Alloys Compd* 421(1–2):166–171. <https://doi.org/10.1016/j.jallcom.2005.09.084>
143. Hegab (2016) Design for additive manufacturing of composite materials and potential alloys: a review. *Manuf Rev* 3(11). <https://doi.org/10.1051/mfreview/2016010>